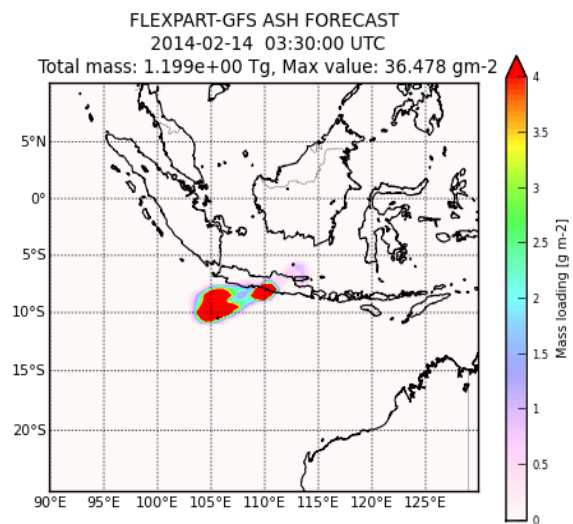
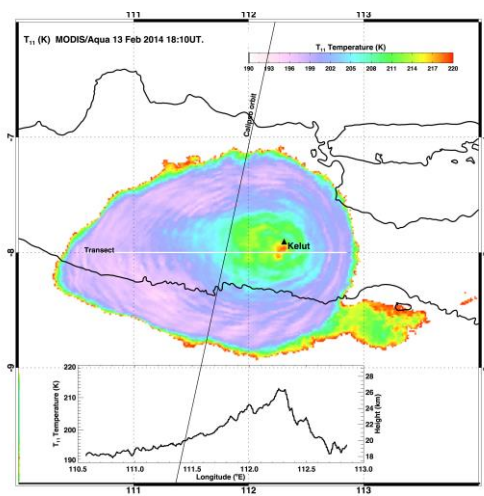


# VAST Volcanic Ash Strategic-initiative Team

## ESA-ESRIN Contract No. 4000105701/12/I-LG

### Final project report



## DOCUMENT STATUS SHEET

	INSTITUTION	NAME	Date	SIGNATURE
LEAD AUTHOR	NILU	Kerstin Stebel	07.02.2016	
CONSORTIUM PARTNER	NILU, now Nicarnica Aviation NILU NILU NILU NILU FMI FMI FMI FMI ZAMG ZAMG ZAMG S[&]T S[&]T NUIG NUIG NUIG NUIG NUIG	Fred Prata Nina Kristiansen Arve Kylling Espen Sollum Andreas Stohl Gerrit de Leeuw Mikhail Sofiev Julius Vira Timo Virtanen Delia Arnold Christian Maurer Gerhard Wotawa Christina Aas Martijn Kamstra Jakub Bialek Maxime Hevro Damien Martin Colin O'Dowd Jana Preißler Răzvan-Cosmin Rădulescu		
ISSUED BY	Project manager	Kerstin Stebel		
REVIEWED BY				
APPROVED BY	Technical officer (ESA)	Claus Zehner		

## EXECUTIVE SUMMARY

From June 2012 to November 2015 the ESA project Volcanic Ash Strategic initiative Team (VAST, [vast.nilu.no](http://vast.nilu.no)) brought together teams from four European countries to improve the quality and use of satellite based observations in numerical atmospheric dispersion models for the purpose of assisting global aviation. The project was set up following recommendations from the ESA Workshop on Monitoring Volcanic Ash from Space (*Zehner, 2012*) and from the European Volcanic Ash Cloud Experts Group (*EVACEG, 2010*) after the eruption of the volcano Eyjafjallajökull in Iceland in April/May 2010, which led to a major disruption of air traffic in Europe, causing total economic damage in the billion-Euro range.

As a follow-on to the 2010 meeting, VAST prepared a review of user requirements (*Aas et al., 2013*) and organized an ESA/EUMETSAT volcanic ash and aviation user workshop in March 2013 in Dublin, Ireland. The Dublin workshop report (*Prata et al., 2014*) summarizes the progress made in the intervening three years on observations and models, as well as on the regulatory side. It showed that, while an event comparable to the eruption of the volcano Eyjafjallajökull in Iceland would be met with a more adaptive and economically effective response, there remain significant challenges to optimize the operational use of satellite, ground and airborne observations during such situations.

VAST was set up to improve the quality and use of space-borne Earth observations. Existing ash and SO<sub>2</sub> retrieval algorithms were improved for a number of satellite instruments: i. Detection and retrieval of volcanic ash from Spinning Enhanced Visible and InfraRed Imager (SEVIRI) measurements (*Prata, 2013*), ii. ash detection from Atmospheric InfraRed Sounder (AIRS) brightness temperatures (*Prata, 2013*), iii. SO<sub>2</sub> and ash retrieval from Moderate Resolution Imaging Spectroradiometer (MODIS) data (*Kylling and Prata, 2013*), and iv. VIS/NIR ash aerosol optical depth (AOD) retrieval (*Virtanen et al., 2013*) and plume top height estimate from the Advanced Along Track Scanning Radiometer (AATSR) (*Virtanen et al., 2013, 2014*).

Near-real time data streams and improved products were set up for SEVIRI (ash detection) and AIRS (SO<sub>2</sub> and ash detection) and both near-real time as well as archived data and images are available online (<http://fred.nilu.no/sat/> and [.../airs/](http://fred.nilu.no/airs/)). The original Volcanic Ash Detection (VOLE) data product, which is running operationally at EUMETSAT, utilises some simple threshold tests for identifying ash affected pixels. The principle among these tests is the BTD (brightness temperature difference). During VAST, an improved cloud identification scheme (CID) was developed, based on more physical principles which eliminates many false detections, thereby resulting in a more reliable volcanic ash product from SEVIRI observations. Furthermore, an AIRS ash detection algorithm, based on the shape of the spectral signature of SiO<sub>2</sub> in the IR wavelengths region, was set up to run automatically in near-real time. The algorithm may be seen as a natural extension of ash detection schemes that rely on 2-channel broadband measurements from imaging instruments such as AVHRR and MODIS. An advantage of the AIRS ash detection algorithm over the 'reverse absorption' (RA) method is its ability to detect ash clouds that are optically thick.

A new volcanic ash aerosol optical depth (AOD) retrieval has been developed on the basis of existing AATSR Dual View (ADV) and AATSR Single View (ASV) ambient aerosol retrieval algorithms. Furthermore, a stereographic ash plume top height estimation method, AATSR Correlation Method (ACM), based on dual-view capability of the AATSR instrument has been developed (*Virtanen et al., 2014*). The Sea and Land Surface Temperature Radiometer (SLSTR) on-board of the recently launched Sentinel-3A satellite has characteristics similar to AATSR, and preparations were made for using the SLSTR data in volcanic ash retrievals (*Virtanen and de Leeuw, 2015*).

As a response to the requirement “R1 Access to all data sources of volcanic plume observations in Europe should be accelerated, improved and open” from Zehner (2012), the VAST team compiled a benchmark test dataset for historic volcanic eruptions. The database is accessible via the [vast.nilu.no](http://vast.nilu.no) website for registered users (*Stebel et al., 2015*). The VAST, the SACS-II (Support for Aviation Control Service), the SMASH (Study on an end-to-end System for volcanic ASH plume monitoring and prediction) teams, individual researchers, as well as research networks provided satellite, model and *in situ* data for the eruption cases of Eyjafjallajökull (2010), Grímsvötn (2011), Kasatochi (2008), Etna (2011), Puyehue-Cordón Caulle (2011), Chaitén (2008), and Mount Kelut (2014).

VAST worked on developing and improving modelling tools used for predicting the transport of volcanic ash and SO<sub>2</sub> in the atmosphere, in particular focusing on incorporating satellite observations into the models in order to obtain more reliable model simulations. Three dispersion models were used: the FLEXible PARTicle dispersion model (FLEXPART), the System for Integrated modeLLing of Atmospheric composition (SILAM), and the Weather Research and Forecasting (WRF) model coupled with Chemistry (WRF-Chem) (*Kristiansen et al., 2014*). The models were used in both research mode and in operational mode.

The main VAST modelling tools were: i. source term inversion used for determining the source term of ash and SO<sub>2</sub> during volcanic eruptions, utilizing satellite observations as a constraint, ii: data assimilation used for correcting errors in the modelled SO<sub>2</sub> transport and input data by updating the modelled SO<sub>2</sub> fields with up-to-date observations, and iii: ensemble modelling used for inferring uncertainties related to the model simulations arising from the meteorological data driving the model, the source term or inherent in the model itself.

As an example, the VAST-inverse modelling tools were applied to the 2014-Kelut eruption (Indonesia) (*Kristiansen et al., 2015*). This particular eruption was given attention due to an accidental aircraft encounter, and it was hoped that modelling could provide an estimate of how much ash the aircraft encountered. It was shown that the combination of satellite observations and modelling was key to obtaining a robust evaluation of this event. As another example, data assimilation method based on the SILAM model and 4D-VAR approaches was developed and tested for a number of cases and compared to the source term inversion estimation method. It was found that model forecasts initialized from the assimilation analysis were less robust than the inversion-driven forecasts mainly due the fact that the column-integrated satellite retrievals provided insufficient information to constrain the plume position vertically within the assimilation. VAST further developed and tested

ensemble Kalman filter (EnKF) techniques based on the SILAM dispersion model, with the aim to construct an assimilation scheme where an ensemble would provide an envelope for the possible plume locations. In addition an ensemble-modelling approach based on the FLEXPART model using ECMWF-ensemble members to perform multiple model simulations taking into account the uncertainty in the meteorological data driving the dispersion model, was set up.

In a model-inter-comparison effort, the Grimsvötn-2011 eruption was used to investigate how well the models used in VAST could simulate the ash clouds (compared to observations), and how the three models differed in terms of ash cloud extent and ash amounts (*Kristiansen et al., 2015*). More validation and inter-comparison results are given in the Product Validation Report (*O'Dowd et al., 2016*).

A demonstration of an operational volcanic ash monitoring and forecasting service was a defining goal of VAST. The operational integration comprises of a dispersion modelling service, an ensemble modelling service, and various post-processing and graphical products. The operational demonstration service operates on a continuous basis for significant volcanic eruptions affecting the European air space and on a best-effort basis for worldwide events. The results are accessible via the [vast.nilu.no](http://vast.nilu.no) website for registered users.

Another of the objectives of VAST was to improve volcanic ash forecasts based on atmospheric dispersion and transport models by a seamless integration of inverse modelling. A dynamic inverse modelling system prototype has been developed with the aim of being run in near-real time providing source term estimates and updated forecasts (*Kristiansen et al., 2014; Arnold et al., 2015*). Further optimization and testing of the system on a near-real time basis is required before its implementation into a fully operational environment. Based on experiences made with a number of case studies, even in an operational dynamical inversion system, it is expected that the results will need some human expert analysis and adjustments in order to provide optimal results.

A LIDAR-observation network in Ireland was seen as beneficial due to its close proximity to the volcanic sources in Iceland, particularly for volcanic aerosol advection in case of westerly and north-westerly winds. The Irish Aviation Authority (IAA) purchased three Raman LIDARs, which unfortunately failed half-way through the VAST project. They were subsequently replaced by two Doppler wind LIDARs. It was demonstrated that the combination of the suite of remote sensing instruments at Mace Head and a Doppler LIDAR at Dublin, enabled the detection of free tropospheric aerosol and its transport over Ireland, a promising result in case of observing future volcanic aerosol transport across Ireland.

Overall, VAST brought together a suite of techniques for aiding aviation in case of volcanic eruptions, including satellite and ground-based observations and modelling approaches. Methods were developed, improved and tested thoroughly, and integrated into an operational demonstration service. ESA support for VAST, as well as the sister-project SACS and SMASH, leaves European institutions and users better prepared to monitor hazardous volcanic ash and SO<sub>2</sub> plumes in the European and global airspace.

## DOCUMENT REVISION

Issue	Date	Modified Items / Reason for Change
0.1	24.04.2014	First draft (TOC) prepared
1.0	29.02.2016	Final draft, including input from project partners

For details about the figure on the front-page, see: Kristiansen, N.I., A.J. Prata, A. Stohl, and S. A. Carn (2015) Stratospheric volcanic ash emissions from the 13 February 2014 Kelut eruption, *Geophys. Res. Lett.*, 42, 588–596, doi:10.1002/2014GL062307.

## List of Acronyms

AATSR	Advanced Along Track Scanning Radiometer
ACM	AATSR Correlation Method
ADV	AATSR Dual View
AIRS	Atmospheric InfraRed Sounder
ATL	Agreement in Threshold Level
AOD	Aerosol Optical Depth
ASV	AATSR Single View
ATBD	Algorithm Theoretical Basis Document
AVHRR	Advanced Very High Resolution Radiometer
BTD	Brightness Temperature Difference
CAA	Civil Aviation Authority
CALIOP	Cloud-Aerosol Lidar with Orthogonal Polarization
CALIPSO	Cloud-Aerosol LIDAR and Infrared Pathfinder Satellite Observation
CID	Cloud Identification Scheme
CTH	Cloud top height
ECMWF	European Center for Medium Range Weather Forecast
EnKF	Ensemble Kalman Filter
ENS	Ensemble Prediction System
ESA	European Space Agency
EO	Earth Observation
EUMETSAT	European Organisation for the Exploitation of Meteorological Satellites
FL	Flight Level
FLEXPART	FLEXible PARTicle dispersion model
FMI	Finnish Meteorological Institute
GOME	Global Ozone Monitoring Experiment
IAA	Irish Aviation Authority
IASI	Infrared Atmospheric Sounding Interferometer
IAVWOPSG	International Airways Volcano Watch Operations Group
ICAO	International Civil Aviation Organisation
IR	Infra-red
LIDAR	Light Detection And Ranging
LUT	Look-up table
MISR	Multi-angle Imaging SpectroRadiometer
MODIS	Moderate Resolution Imaging Spectroradiometer
MSG	Meteosat Second Generation
MTG	Meteosat Third Generation
NASA	National Aeronautics and Space Administration
NILU	Norwegian Institute for Air Research
NIR	Near Infra-red
NOTAM	NOTice To AirMen
NUIG	National University of Ireland, Galway
NRT	Near-real time
OMI	Ozone Monitoring Instrument
RA	reverse absorption



SACS	Support for Aviation Control Service
SAVAA	Support to Aviation for Volcanic Ash Avoidance
SCIAMACHY	SCanning Imaging Absorption spectroMeter for Atmospheric CHartographY
SEVIRI	Spinning Enhanced Visible and Infrared Imager
SILAM	System for Integrated modelLing of Atmospheric composition
SLSTR	Sea and Land Surface Temperature Radiometer
SMASH	Study on an end-to-end System for volcanic ASH plume monitoring and prediction
SO <sub>2</sub>	Sulfur dioxide
TIR	Thermal Infra-red
UTLS	Upper Troposphere - Lower Stratosphere
UV	Ultra-violet
URD	User Requirement Document
VAST	Volcanic Ash Strategic-initiative Team
VAAC	Volcanic Ash Advisory Centre
VIS	Visible
WMO	World Meteorological Organization
WRF-Chem	Weather Research and Forecasting (WRF) model coupled with Chemistry
ZAMG	Zentralanstalt für Meteorologie und Geodynamik



## LIST OF FIGURES

Figure 2-1: Main obstacles to adopt the use of new/additional EO data products. ....	13
Figure 3-1: Brightness temperature difference image at 11-12 $\mu\text{m}$ (upper panel) .....	15
Figure 3-2: Histogram of CID pixels identified by each of the tests. ....	16
Figure 3-3: Ash mass loading (upper left), error in ash mass loading .....	16
Figure 3-4: Ash mass loadings ( $\text{gm}^{-2}$ ) for an ash cloud from Puyehue-Cordón Caulle.....	17
Figure 3-5: The ash mass loading from the Grimsvötn 2011 eruption.....	19
Figure 3-6: AATSR ash detection (BTD) and mass load retrieval on May 6, 2010. ....	20
Figure 3-7: ACM plume top height (left) compared to the mean FLEXPART height.....	21
Figure 3-8: Plume top height for ash-affected pixels from operational satellite data. ....	22
Figure 4-1: IASI satellite observations (left panel) of $\text{SO}_2$ (top) and ash .....	24
Figure 4-2: Kelut-2014.....	25
Figure 4-3: Kelut-2014 modelled ash cloud.....	26
Figure 4-4: Steps of source inversion and assimilation analysis procedures.....	27
Figure 4-5: Comparison of the total columns and zonal means of $\text{SO}_2$ concentrations....	27
Figure 4-6: Spatial correlation coefficient .....	28
Figure 4-7: EnKF simulations .....	29
Figure 4-8: Comparison of EnKF analysis (upper row) with OMI.....	30
Figure 4-9: Maximum concentration (left panel) and ATL plot (right panel) for FL 300...	31
Figure 4-10: Grimsvotn-2011 modelled ash cloud simulated .....	32
Figure 4-11: Grimsvotn-2011 modelled ash cloud simulated .....	33
Figure 5-1: AATSR top ash plume heights (red circles) superimposed over FLEXPART ...	34
Figure 5-2: Right: Validation of a posteriori model simulations .....	35
Figure 6-1: Example of database page .....	37
Figure 7-1: VAST project website (main page). ....	38
Figure 7-2: NRT SEVIRI ash detection analysis using new CID scheme.....	39
Figure 7-3: NRT and archived AIRS $\text{SO}_2$ retrieval and ash detection for selected areas. .	40
Figure 8-1: VAST website overview of events.....	42
Figure 8-2: Example of the model forecasts .....	43
Figure 8-3: 2D output from the operational mini multi-input ensemble modelling .....	44
Figure 8-4: Time-height output from the operational mini multi-input ensemble.....	44
Figure 8-5: Diagram of the dynamic inversion system .....	45
Figure 9-1: Vertical profiles of the backscattered signal on 21 February 2015. ....	47
Figure 9-2: Backscattered signal from N-S scan over zenith on 21 February 2015 .....	48
Figure 9-3: Feature mask on 19 April 2010, after the eruption of Eyjafjallajökull. ....	48

## TABLE OF CONTENTS

<b>DOCUMENT STATUS SHEET .....</b>	<b>2</b>
<b>EXECUTIVE SUMMARY .....</b>	<b>3</b>
<b>LIST OF ACRONYMS.....</b>	<b>7</b>
<b>LIST OF FIGURES .....</b>	<b>9</b>
<b>1. INTRODUCTION.....</b>	<b>11</b>
<b>2. USER REQUIREMENTS AND THEIR UPDATES .....</b>	<b>12</b>
2.1 USER REQUIREMENTS .....	12
2.2 USER WORKSHOP REPORT.....	13
2.3 USER FEEDBACK .....	14
<b>3. SATELLITE ALGORITHM DEVELOPMENT .....</b>	<b>14</b>
3.1 DETECTING AND RETRIEVING VOLCANIC ASH FROM SEVIRI .....	14
3.2 VOLCANIC ASH DETECTION USING AIRS BRIGHTNESS TEMPERATURES .....	17
3.3 DETECTION AND RETRIEVING VOLCANIC ASH AND SO <sub>2</sub> FROM MODIS .....	18
3.4 AATSR VIS/NIR AOD RETRIEVAL.....	19
3.5 AATSR PLUME TOP HEIGHT ESTIMATE.....	21
3.6 USE OF OPERATIONAL EO DATA PRODUCTS .....	22
3.7 PREPARATION FOR SLSTR .....	22
<b>4. MODELLING DEVELOPMENT .....</b>	<b>23</b>
4.1 INVERSE MODELLING.....	23
4.2 DATA ASSIMILATION .....	26
4.3 ENSEMBLE MODELLING .....	28
4.3.1 Ensemble Kalman Filter as a source inversion technology .....	29
4.3.2 Multi-input ensemble using ECMWF meteorological ensembles .....	30
4.4 MODEL INTER-COMPARISON .....	32
<b>5. VALIDATION AND INTERCOMPARISON .....</b>	<b>33</b>
<b>6. DATABASE FOR HISTORICAL ERUPTIONS.....</b>	<b>36</b>
<b>7. DOCUMENTATION AND DATA ACCESS .....</b>	<b>38</b>
7.1 PROJECT WEBPAGE.....	38
7.2 NRT SATELLITE BASED ASH DETECTION, SO <sub>2</sub> , AND MODEL RESULTS.....	38
<b>8. OPERATIONAL DEMONSTRATION SERVICE .....</b>	<b>41</b>
8.1 OPERATIONAL MODEL FORECASTING SERVICE.....	41
8.2 OPERATIONAL ENSEMBLE MODELLING SERVICE.....	43
8.3 DYNAMICAL INVERSE MODELLING SYSTEM.....	44
8.4 EMAIL NOTIFICATION SERVICE.....	45
<b>9. THE IRISH LIDAR ASH DETECTION NETWORK .....</b>	<b>47</b>
<b>9. CONCLUSIONS AND OUTLOOK .....</b>	<b>49</b>
<b>10. BIBLIOGRAPHY.....</b>	<b>51</b>
<b>REFERENCES .....</b>	<b>52</b>

## 1. INTRODUCTION

In April and May 2010, large parts of the European airspace were shut down for several days as a consequence of the eruption of the volcano Eyjafjallajökull in Iceland. The total financial impact of the event has been estimated at € 5 billion (*Oxford Economics, 2010*). The significant economic impact and public awareness of these air traffic restrictions raised the need to promote initiatives aimed at improving the management of volcanic eruptions in the context of civil aviation. Besides the aviation issues, volcanic ash can, on a larger scale, also affect human health and agriculture.

The problem of transport of ash and its interaction with aviation is a global problem (*Prata, 2008*), and requires a global approach. Satellite data (earth observation data, referred to hereafter as EO data) is best suited for ash detection and observation because of its global perspective, timeliness and in the case of volcanoes because it presents no risk during acquisition. During and after the Eyjafjallajökull eruption, the European Space Agency (ESA) convened a meeting in Frascati to investigate better ways to utilize EO data for monitoring and forecasting volcanic ash. The group consisted of experts from many European countries but also included international experts. The report of the meeting (*Zehner, 2012*) provided a timely and valuable set of recommendations, the following of which were relevant for VAST:

- Access to all data sources for volcanic plume observations, in particular R1.6 for the generation of a data-base of measurements for the April/May eruptions of Eyjafjallajökull.
- Consolidation of EO observations and other ground-based data for characterising volcanic ash clouds (R2).
- Development of operational volcanic ash products from EO data using advanced retrieval algorithms (R4).
- Further development of dispersion forecast models (global and regional) including data assimilation, inverse modelling, and ensemble techniques to generate a measure of uncertainty of the forecast (R5).
- Availability of real-time monitoring (including satellite data) of the dispersion processes, which is fundamental for the confirmation (validation) or confutation (verification) of model predictions (R6).
- Performance of periodic model inter-comparison/evaluation exercises on volcanic eruptions that should involve Volcanic Ash Advisory Centres (VAACs), meteorological services, volcano observatories and other volcanology institutes with operational forecasting capabilities in Europe that are used in support of decision making at the national level (R10).
- Integration and management of data by the running VAACs as part of International Airways Volcano Watch Operations Group (IAVWOPSG) within ICAO, and providing additional European modelling capability as part of a multi-model ensemble prediction system (R10).

The ESA project VAST was established involving teams from four European countries to improve the quality and use of EO based observations in numerical atmospheric dispersion models for the purpose of assisting global aviation. VAST proposed a demonstration services that includes modeling services,

improved satellite retrievals, improved volcanic ash source term estimates, other data services and assessment services, based on the use of several different dispersion models including: FLEXible PARTicle dispersion model (FLEXPART), System for Integrated modelLing of Atmospheric composition (SILAM), and Weather Research and Forecasting (WRF) model coupled with Chemistry (WRF-Chem). The FLEXPART model was used in both research mode (at NILU) and in an operational mode (at ZAMG in Vienna). The demonstration of an operational volcanic ash monitoring and forecasting service was a defining goal of this project.

## 2. USER REQUIREMENTS AND THEIR UPDATES

### 2.1 User requirements

As part of the preparation of a User Survey, the existing user requirements were reviewed:

- Support to Aviation for Volcanic Ash Avoidance (SAVAA) requirements dating from April, 2009: Focused especially on the needs of the London and Toulouse VAACs, as these were key stakeholder users of the SAVAA project.
- Recommendations from ESA-EUMETSAT workshop, May, 2010 (*Zehner, 2012*).
- VAAC requirements.

In total 74 entities responded to a user survey, which was set up by S[&]T. 62 % of users responding to the survey were from research (45 responses) and 38% from operational (29 responses) institutions. Seven out of nine VAACs, three airlines (KLM, Icelandair, Qantas airways), regulative authorities (EASA, Irish Aviation Authority, Civil Aviation Authority – International Civil Aviation Organisation (CAA-ICAO), air traffic services operators, pilots, and meteorologists replied. The results are summarized in the User Requirements Document (URD) (*Aas et al., 2012*). Key findings were:

- **Existing volcanic hazard products:** The slight majority of the operational users make use of the VAAC warnings as well as the Support for Aviation Control Service (SACS) service products. The results were fairly similar for the research users except that the slight majority makes use of research satellite products.
- **Main obstacles for adopting new/additional EO products:** For the operational users the main obstacle is the too long product delivery time, whereas for the research users the main obstacle is the sufficiency of the spatial and temporal resolution (see *Figure 2-1*).
- **Product delivery:** Both the operational and the research users preferred the internet or email as the main delivery mechanisms for ash alerts and products.
- **Horizontal spatial resolution:** research users have more stringent requirements (0.5-1 km versus 5-10 km for operational users). The previous requirement from the SAVAA project: 1 km.
- **Minimum spatial accuracy:** For the operational users the minimum acceptable spatial accuracy of satellite-based products (both volcanic cloud dispersion and SO<sub>2</sub> retrieval) was

less than 10 km, whereas the majority of the research users selected a minimum acceptable spatial accuracy of less than 1 km.

- **Product timeliness:** research users have less stringent requirements (2 hours update frequency versus 30 minutes requirement for operational users). For SAVAA this was 15 minutes.
- **Dispersion model timeliness:** the research users required the model forecast products to be available less than 1 hour after eruption, whereas operational users require availability after 15 minutes. From the SAVAA project the requirement was: less than 1 hour.

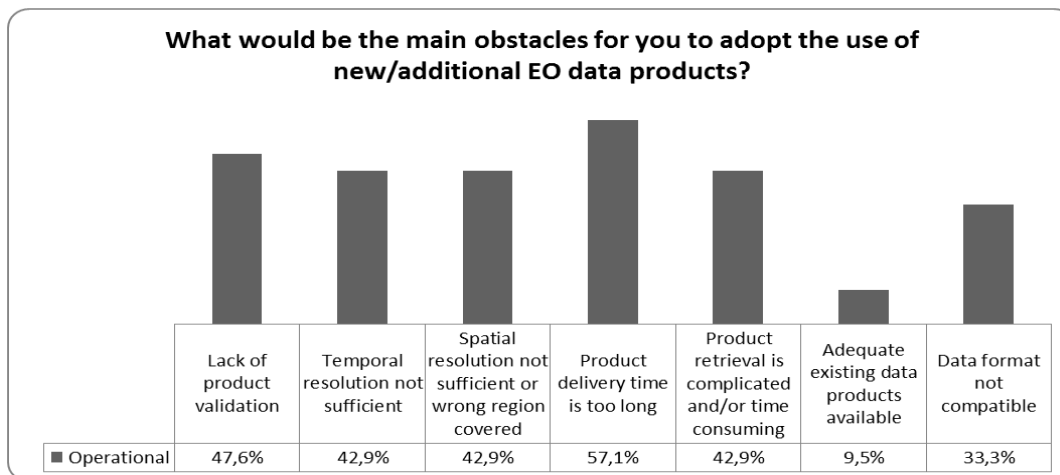


Figure 2-1: Main obstacles to adopt the use of new/additional EO data products.

## 2.2 User workshop report

A follow-on to the 2010 meeting an ESA/EUMETSAT volcanic ash and aviation user workshop was organized by VAST in March 2013 in Dublin, Ireland (for details and presentations see <http://vast.nilu.no/meetings/workshops/dublin2013/>). This brought together representatives of the research community along with aircraft manufacturing industry, airline operators, regulators and meteorological offices, to review progress and guide on-going work within VAST. The Dublin workshop report (*Prata et al., 2014*) summarized the workshop findings on progress made in the intervening three years on observations and models, as well as on the regulatory side. It showed that, while an event comparable to the eruption of the volcano Eyjafjallajökull in Iceland, would be met with a more adaptive and economically effective response, there remains significant opportunity to optimize the operational use of satellite, ground and airborne observations during such situations. Furthermore, the Dublin workshop report includes a Table highlighting the progress made on the main recommendations from *Zehner (2012)*. One aspect the authors highlighted, was that validation data for volcanic ash are sparse and the outstanding need for validation of satellite based volcanic ash retrievals.

In June 2015, World Meteorological Organization (WMO) organized an *Inter-comparison of Satellite-based Volcanic Ash Retrieval Algorithm Workshop* ([http://cimss.ssec.wisc.edu/meetings/vol\\_ash15/](http://cimss.ssec.wisc.edu/meetings/vol_ash15/))

in Madison WI, USA. 26 ash algorithms took place in the inter-comparison exercise, including the Advanced Along Track Scanning Radiometer (AATSR) retrieval from FMI (see chapter 3.4 AATSR VIS/NIR AOD Retrieval).

## 2.3 User feedback

Service Level Agreements with VAST were signed with Aer Lingus, MET Norway and AVINOR. AVINOR is a wholly-owned state limited company under the Norwegian Ministry of Transport and Communications and is responsible for 46 state-owned airports. AVINOR has the responsibility for defining the areas with high and medium ash concentration in the Norwegian air-space, based on information from the VAAC and National competence (MET Norway and NILU). They issue NOTAMs for those areas. MET Norway does its own evaluations of ash dispersion in the Norwegian air space and inform the airlines about the weather situations in the areas with low ash concentration.

In their user feedback, AVINOR and MET.NO confirmed that the information and products from VAST were relevant and useful to them. VAST services could provide additional information that would be beneficial in the assessment of a potential future ash 'crisis' situation over Norway.

## 3. SATELLITE ALGORITHM DEVELOPMENT

The ESA project VAST aimed to improve the quality and use of EO based observations in numerical atmospheric dispersion models. The advances made in terms of satellite observations are summarized below.

### 3.1 Detecting and Retrieving Volcanic Ash from SEVIRI

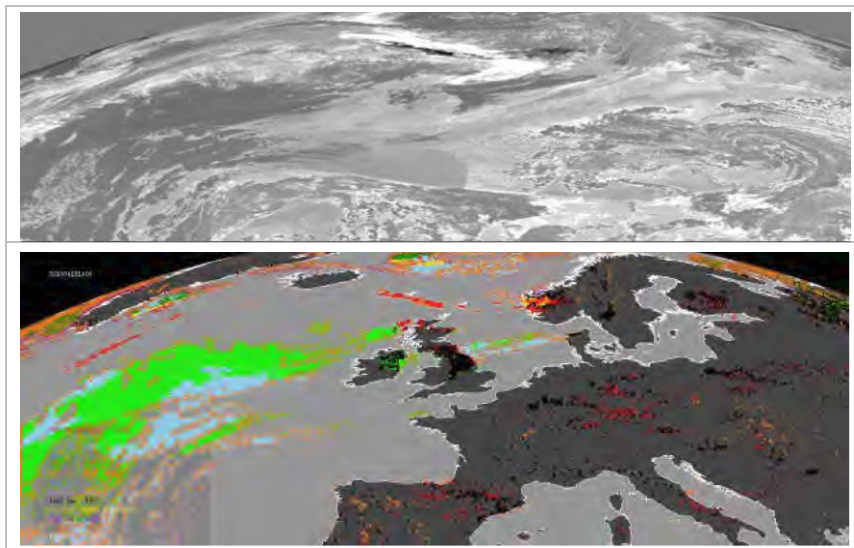
An improved volcanic ash retrieval scheme based on data from the geostationary, Meteosat Second Generation (MSG) Spin-stabilised Enhanced Visible and InfraRed Imager (SEVIRI) is described in the Algorithm Theoretical Basis Document (ATBD), see *Prata (2013)*. **Algorithmic improvements**, development of an improved **cloud identification scheme (CID)**, and the **validation** of the retrievals, are addressed in the document. The algorithm utilises the infrared channels of SEVIRI to provide retrievals of mass loading, effective particle radius and infrared optical depth at pixel scale every 15 minutes. Look-up tables (LUTs), generated off-line are used to convert the brightness temperatures to the basic retrieved quantities, infrared optical depth and effective particle radius, after identifying a pixel as containing volcanic ash. The LUTs can be updated as required and rely on spectral refractive index data and estimates of cloud-top and surface temperatures.

The original Volcanic Ash Detection (VOLE) data product, which was developed for EUMETSAT (<http://navigator.eumetsat.int/discovery/Start/DirectSearch/DetailResult.do?f%28r0%29=EO:EUM:D AT:MSG:VOLE>) is based on the reversed split window technique, and utilises a simple threshold test to identify ash affected pixels. The principle among this test is the BTD (brightness temperature difference), which states that:  $BTD = T_{11} - T_{12} < \Delta T_0$ , where  $T_{xx}$  are the brightness 11  $\mu\text{m}$  and 12  $\mu\text{m}$

brightness temperature, and  $\Delta T_0$  the BTD threshold, theoretically taken to be 0 K. As discussed in Prata et al. (2001) the threshold of 0 K can lead to so-called falls-positive, therefore an approach is to set  $T_0 < 0$  K, e.g. at -0.5 K, which implies then a risk of elimination of valid ash identifications, so called false-negatives.

Within VAST a new series of tests for an improved **cloud identification scheme (CID)**, based on physical principles, have been developed. Additional tests are implemented, taking account for the pixel location (over land/sea, and zenith angle) and the effects of clouds and water vapor as well as  $SO_2$ . These additional tests are making use of additional channels. While these tests eliminate many false detections, there is still no method of cloud detection that can be regarded as complete.

In *Figure 3-1* (upper panel) the 'standard' BTD is used to identify the ash cloud, which in this case is most likely also obscured by water and ice clouds. The CID scheme implements a further 11 tests in attempt to better identify pixels that are ash contaminated, or more aptly, remove pixels that are not ash contaminated. *Figure 3-1* (lower panel) shows the CID scheme for the image of 15 April, 2010 at 14:00 UTC.



*Figure 3-1: Brightness temperature difference image at 11-12  $\mu\text{m}$  (upper panel). The scale ranges from -3 K (black) to 3 K (white). Ash clouds appear black. Lower image: CID image with colours identifying which tests have been flagged for each pixel. Pixels coloured red are finally identified as containing ash. Note that some pixels over land are misidentified as ash. The colour legend may be found in Figure 3-2.*

The CID tests presented (see Table 5.1 on page 40 of the ATBD) are determined for just a few cases including Eyjafjallajökull, Grimsvötn and Puyehue and show satisfactory results for these cases. *Figure 3-2* provides a summary of the CID pixels as a per cent of the total number of pixels. The most notable observation is that the ash affected pixels is less than 0.5 % of the total, while it is down by more than a factor 10 over the 'standard' BTD method (see *Figure 3-1*). Clouds overwhelm the pixel identification (test 11).

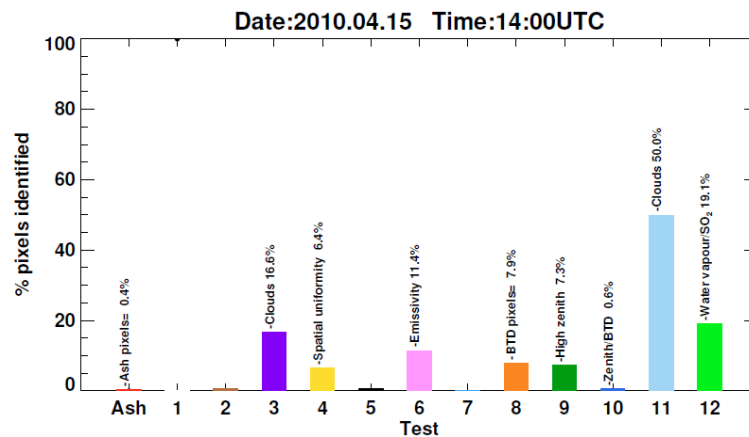


Figure 3-2: Histogram of CID pixels identified by each of the tests. The percentage represent pixels identified by the test out of the total image pixels. Note: the sum exceeds 100%, because different tests are satisfied by the same pixels.

An example of ash retrieval for the Eyjafjallajökull eruption is shown in Figure 3-3. Validation of the scheme using data for two volcanic eruptions suggest that under favourable conditions the lower limit for mass loading retrieval is  $0.2 \text{ gm}^{-2}$ . (Prata and Prata, 2012). A validation data-set derived for Eyjafjallajökull can be downloaded from the VAST database.

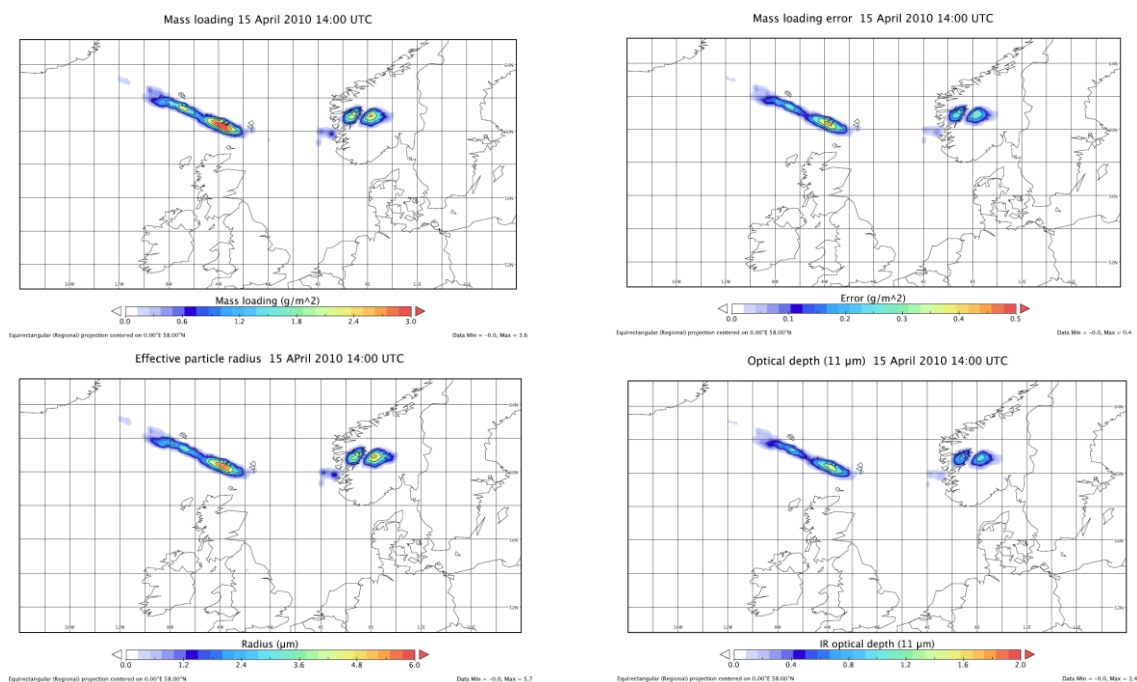


Figure 3-3: Ash mass loading (upper left), error in ash mass loading (upper right), effective particle radius (lower left), and IR optical depth (lower right) retrieval after using CID – only ash identified pixels (“red” coloured ones in Figure 3-1) have been processed in the retrieval. A 3x3 pixel spatial filter has also been applied, which efficiently removes isolated pixels, especially those misidentified over land.

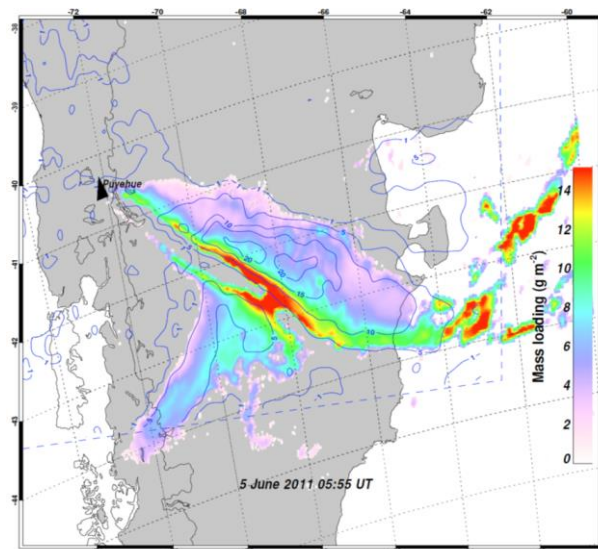


### 3.2 Volcanic Ash Detection Using AIRS Brightness Temperatures

A volcanic ash detection algorithm using Atmospheric InfraRed Sounder (AIRS) brightness temperatures is described in *Prata (2013)*. A simple algorithm based on brightness temperature differences derived from the AIRS instrument (Chahine et al., 2006) is developed. The algorithm relies on the shape of the spectral signature of SiO<sub>2</sub> in the IR wavelengths region. The algorithm may be seen as a natural extension of ash detection schemes that rely on 2-channel broadband measurements from imaging instruments such as AVHRR and MODIS.

AIRS radiances available on a granule basis are converted to brightness temperatures. From the available channels, 12 are selected and averaged to form four "ash" channels. The "ash" channels are combined to give a single brightness temperature difference, as follows,  $\Delta T_a = BT_1 - BT_2 + BT_3 - BT_4$ . The ash detection criterion,  $\Delta T_a > \Delta T_c$  identifies an ash affected pixel and issues an alert for that pixel. The basis behind this idea is provided in the papers by Gangale et al. (2010) and Clarisse et al. (2010) and has been termed the 'concavity' effect. To eliminate "false" detections due to desert sand, a temperature threshold  $BT_1 < T_h$  is included, where  $T_h$  is a temperature cut-off for to eliminate "hot" pixels. A threshold for  $\Delta T_a = 2K$  and  $T_h = 290 K$  were found to work well; for details see *Prata (2013)*.

An advantage of the AIRS ash detection algorithm over the 'reverse absorption' (RA) method is its ability to detect ash that is optically thick. In the RA method the brightness temperature difference tends to go towards zero for optically thick clouds ( $\tau_{10.8} \sim 3.0$ ). This is illustrated by a comparison of MODIS and AIRS in *Figure 3-4* for the initial ash-rich eruption of Puyehue-Cordón Caulle on 4 June, 2011.



*Figure 3-4: Ash mass loadings ( $gm^{-2}$ ) for an ash cloud from Puyehue-Cordón Caulle, Chile, on 5 June 2011 at 05:55 UT, retrieved from MODIS/Aqua infrared brightness temperatures and a radiative transfer model (colours) and AIRS ash detection  $\Delta T_a$ 's (blue contours). Note the central red-coloured portion of the ash cloud indicates saturation in the MODIS retrieval but not in the AIRS ash detections.*

### 3.3 Detection and Retrieving Volcanic Ash and SO<sub>2</sub> from MODIS

The algorithm for detection and retrieval of volcanic ash and SO<sub>2</sub> from the Moderate Resolution Imaging Spectroradiometer (MODIS) infrared window region channels is described in *Kylling and Prata (2013)*. MODIS data are downloaded from NASA DAACs (<http://ladsweb.nascom.nasa.gov/>) or from the NRT “rapid fire” website service (<http://earthdata.nasa.gov/data/near-real-time-data/rapid-response>). Radiances are recovered from scaled integers, and are converted to brightness temperatures as described in the MODIS Swath-to-Grid Toolbox (<http://nsidc.org/data/modis/ms2gt/>).

Volcanic ash information is obtained from MODIS infrared measurements in two separate steps. Identification of pixels containing ash is based on the reverse absorption technique (*Prata, 1989*). In a second step, ash mass loading and effective ash particle radius is determined for these pixels. Ash particle optical properties are calculated with a Mie program assuming spherical particle shape.

In the TIR SO<sub>2</sub> absorption can be seen in the  $\nu_1$ -band, between 1160–1290 cm<sup>-1</sup> (8.62–7.75  $\mu\text{m}$ , channel 29), and the  $\nu_3$ -band, between 1330–1390 cm<sup>-1</sup> (7.52–7.19  $\mu\text{m}$ , channel 28). The SO<sub>2</sub>  $\nu_3$ -band is significantly stronger than the  $\nu_1$ -band, but there is also greater water vapour absorption across the  $\nu_3$ -band. For SO<sub>2</sub> the 7.3  $\mu\text{m}$  and 8.6  $\mu\text{m}$  bands are used to estimate SO<sub>2</sub> concentrations. Details and description of the 8.6  $\mu\text{m}$  band algorithm are found in the SAVAA ATBD (*Prata and Corradini, 2009*). It was generally believed that water vapour absorption would make it difficult to determine SO<sub>2</sub> from broadband measurements in the  $\nu_3$ -band. Above 5 km or so there is less than 5% of the total precipitable water, based on global climatological considerations. Consequently, broadband measurements of the excess absorption of 1362 cm<sup>-1</sup> (7.34  $\mu\text{m}$ ) infrared radiation in the Upper Troposphere - Lower Stratosphere (UTLS) can be used to infer SO<sub>2</sub> concentrations. The VAST ATBD describes the retrieval of SO<sub>2</sub> from the  $\nu_3$ -band. The contribution to the absorption by the background atmosphere is calculated using MODIS IR channels with band centres that lie below (channel 27 centred near 1477 cm<sup>-1</sup>) and above (channel 32 centred near 831 cm<sup>-1</sup>) the 1362 cm<sup>-1</sup> channel. For each MODIS image the radiance at 1362 cm<sup>-1</sup> can be estimated by linearly interpolating the radiances at 1477 cm<sup>-1</sup> and 831 cm<sup>-1</sup>. When there is excess absorption in the 1362 cm<sup>-1</sup> channel, the difference between the estimated 1362 cm<sup>-1</sup> radiance and the actual 1362 cm<sup>-1</sup> radiance is due to the presence of SO<sub>2</sub>. Examples of ash mass loading from the Grimsvötn 2011 eruption as estimated from MODIS are given in *Figure 3-5*.

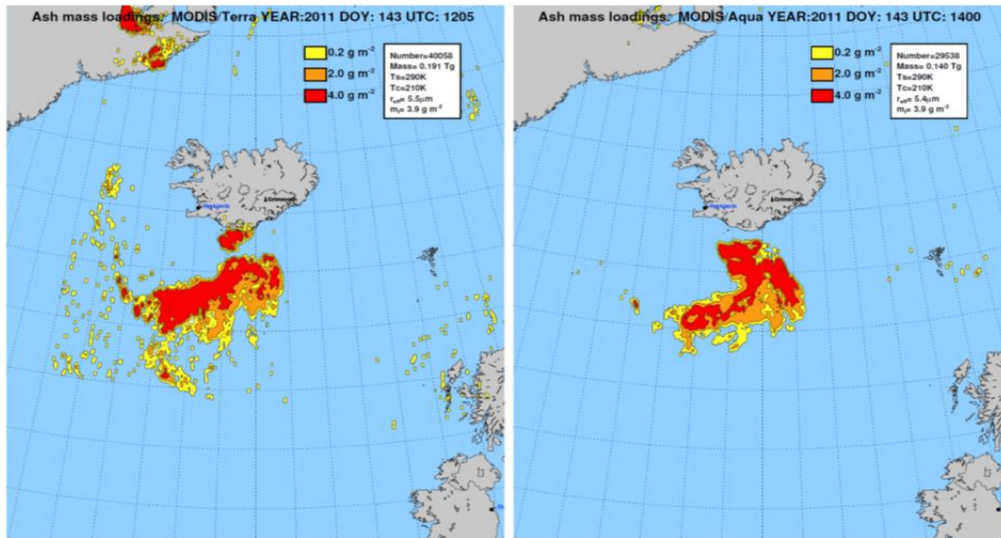


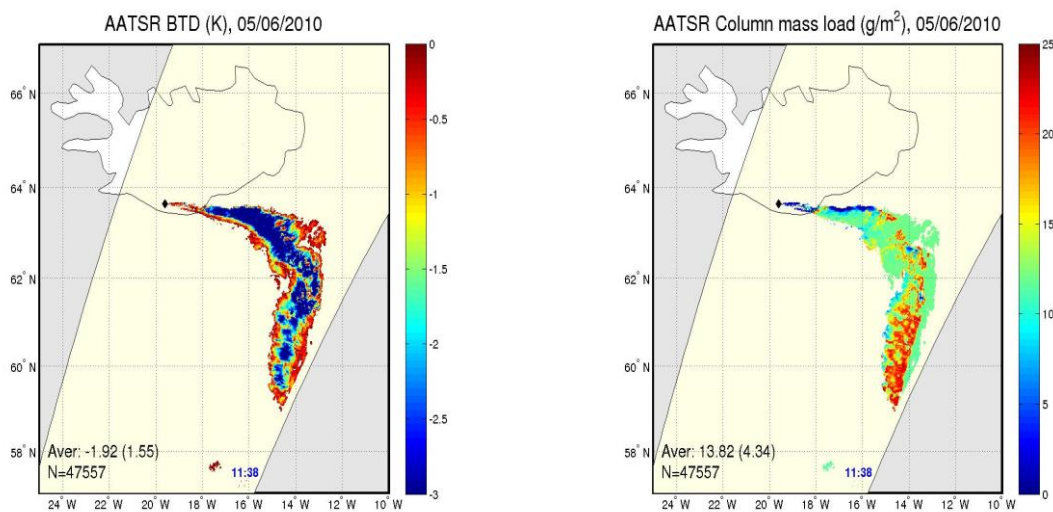
Figure 3-5: The ash mass loading from the Grimsvötn 2011 eruption as estimated from MODIS on board Terra (left plot, 23 May, 1205 UTC) and Aqua (right plot, 23 May, 1400 UTC).

### 3.4 AATSR VIS/NIR AOD Retrieval

An ash retrieval algorithm for visible (VIS) and near-infrared (NIR) AATSR data has been developed and implemented during the VAST project. The work is based on the existing AATSR Dual View (ADV) and AATSR Single View (ASV) ambient aerosol retrieval algorithms (Kolmonen *et al.*, 2015), which have been adapted to ash-specific retrievals. The details of the improved algorithm are described in the AATSR VIS/NIR AOD Retrieval Algorithm Theoretical Basis Document (Virtanen *et al.*, 2013).

The method is based on top of atmosphere measurements of solar radiation reflected from the atmosphere and surface. The surface reflectance is eliminated by using an ocean surface reflectance model, or using the dual-view capability of AATSR over land surfaces. The remaining atmospheric reflectance is then matched with pre-calculated aerosol look-up-tables (LUTs), which give the best fitting aerosol model parameters: aerosol optical depth (AOD) and aerosol mixture. AOD is then converted to column mass load values using an estimated particle size distribution and ash density. For ash-specific retrievals, new aerosol models based on the refractive indexes of andesite (Pollack *et al.* 1973), have been implemented. The algorithm has been adjusted to allow for a semi-free retrieval of the effective radius of ash particles. For ash detection the thermal infrared (TIR) channels centered at 10.85  $\mu\text{m}$  and 12  $\mu\text{m}$  were utilized, following the brightness temperature difference or reverse absorption technique (Prata 1989). Investigations on the use of visible wavelength channels for ash detection were performed, but proved to be too unreliable for operational use.

In visible wavelength aerosol retrievals the presence of water or ice clouds lead to erroneous results, and clouded scenes need to be removed before retrieval. The cloud screening methods generally used in ADV/ASV algorithm have been adjusted for ash plume retrievals. Since the standard cloud screening methods tend to remove all ash plumes, a new approach was developed, where ash retrieval is attempted for all ash-flagged pixels, and an ad-hoc cloud mask is applied as post-processing. AATSR retrieval results for six eruptions (Puyehue-Cordón Caulle, Eyafjallajökull, Grímsvötn, Kasatochi, Chaiten, and Etna) are available in the VAST database (see <http://vast.nilu.no/test-database/>). An example of AATSR ash detection and retrieval is shown in *Figure 3-6*.



*Figure 3-6: AATSR ash detection (BTD) and mass load retrieval on May 6, 2010. Negative brightness temperature difference (BTD) is a sign of volcanic ash, but is not directly proportional to the column mass loading.*

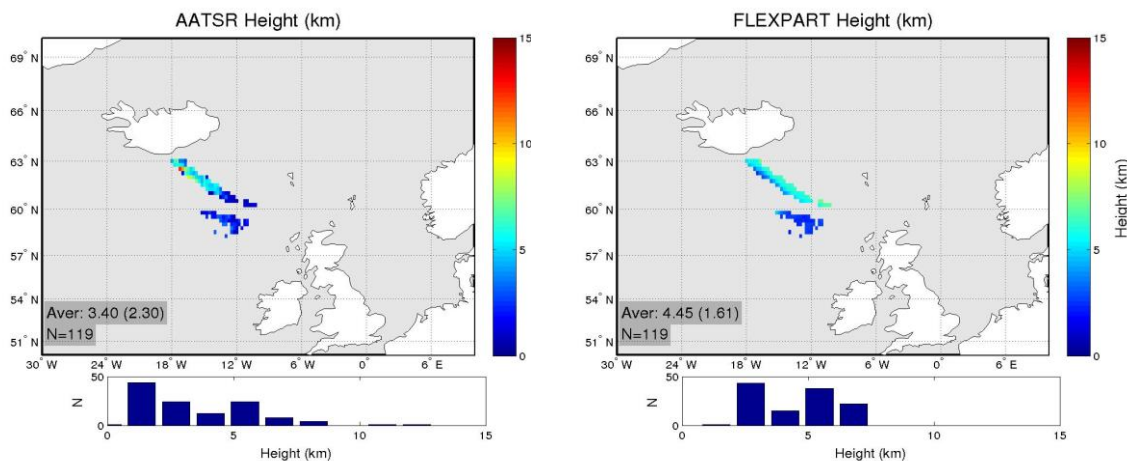
FMI participated in the WMO Inter-comparison of Satellite-based Volcanic Ash Retrieval Algorithm Workshop ([http://cimss.ssec.wisc.edu/meetings/vol\\_ash15/](http://cimss.ssec.wisc.edu/meetings/vol_ash15/)) in June 2015 with AATSR data. The comparison showed that there is variation in the results between the 26 participating algorithms using various satellite instruments. The AATSR AOD values correlated relatively well with Oxford ORAC results, which also use visible wavelengths. The AATSR VIS/NIR results were also compared with FLEXPART dispersion model results and SEVIRI thermal infrared (TIR) retrievals within VAST (Product Validation Report, *O'Dowd et al., 2016*). The comparison shows that the mass loads from VIS/NIR retrievals are much higher than those from the TIR retrievals, in agreement with the WMO report. This reflects the fact that the two methods are sensitive to different particle sizes.

Limitations of the VIS/NIR ash retrieval method were identified during the project. It was discovered that the stereo-view retrieval method used over land is unreliable for very thick ash plumes. The results are still reported over land, but a quality flag is given, instructing the user not to rely on the over land results. It was also noticed that while the primary retrieval result, AOD, is not very sensitive to the aerosol models selected for the retrieval, the conversion to mass load depends largely on the pre-selected aerosol size distribution parameters. With the limited apriori knowledge of the actual size

distribution of volcanic ash, this causes uncertainty in the mass loads retrieved with the VIS/NIR wavelengths.

### 3.5 AATSR Plume Top Height Estimate

A stereographic ash plume top height estimation method, AATSR Correlation Method (ACM), based on dual-view capability of the AATSR instrument has been developed. AATSR measures the radiation from the same location twice, first at a 55° forward angle and two minutes later at nadir. Comparing two images of the same area from different angles with photogrammetric methods allows the estimation of plume top heights with a nominal vertical resolution of 1 km. The AATSR aerosol retrieval and plume top height retrieval are performed simultaneously in a single combined algorithm, using the same ash mask. This allows for simultaneous retrieval of information on both the horizontal and vertical distribution of ash with 1 km horizontal resolution. The method is described in *Virtanen et al. (2014)* and in the AATSR Plume Top Height Estimate Algorithm Theoretical Basis Document (*Virtanen and de Leeuw, 2013*). Example of the height retrieval results is shown in *Figure 3-7*.



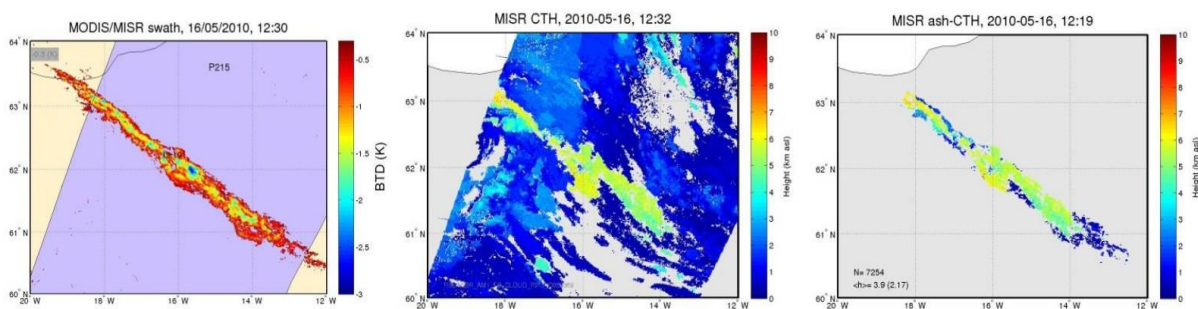
*Figure 3-7: ACM plume top height (left) compared to the mean FLEXPART height (center of mass) on 16/05/2010.*

The ACM height estimate has been compared with plume top height data from the space-borne LIDAR CALIOP, stereo-view satellite instrument MISR, web-camera imagery, and weather radars close to the Eyjafjallajökull volcano, and the method principle was validated against topographic data (*Virtanen et al., 2014*). All comparisons showed reasonable performance. In the WMO inter-comparison exercise the AATSR height estimates compared relatively well with NOAA MODIS algorithm. Comparison with the FLEXPART dispersion model results shows good agreement close to the plume source (Product Validation Report, *O'Dowd, 2016*). Although the comparisons show reasonable agreement in most cases, further development of ACM is needed for example in multilayer cases.

### 3.6 Use of operational EO data products

The use of the operational products from two NASA EO instruments, MODIS and MISR, for ash detection and plume top height estimation has been studied. Since the development teams for these instruments were not included in the project, no tailored products were developed, and only the use of existing data products has been evaluated. The results are described in the Report on the use of operational EO data, *Virtanen and de Leeuw (2015)*.

With two instruments and a 2330 km swath width MODIS provides daily global coverage on 36 spectral bands. Simple treatment of the operational brightness temperature products allows ash detection using the reverse absorption technique (*Prata 1989*). MISR is a stereo-viewing instrument with nine views and four bands in the UV/VIS range, and provides an operational cloud top height product. Although MISR lacks the TIR channels for ash detection, its placement on the same platform (Terra) with one of the MODIS instruments enables the acquiring of ash plume top height estimates. The MODIS ash mask can be used to limit the operational MISR cloud top height (CTH) estimate results to the area affected by ash. An example showing plume top height for ash-affected pixels using operational MODIS and MISR data is shown in *Figure 3-8*.



*Figure 3-8: Plume top height for ash-affected pixels from operational satellite data. Left: MODIS BTM used for ash detection, the violet shade shows the MISR swath. Center: MISR cloud top height product. Right: combined data: MISR CTH for ash-masked pixels only.*

### 3.7 Preparation for SLSTR

Connection to ENVISAT platform carrying the AATSR instrument was lost in April 2012, just months before VAST started. While the existing AATSR data archives were available for off-line research, preparations for the use of the follow-up instrument, the Sea and Land Surface Temperature Radiometer (SLSTR), within VAST were started. SLSTR has characteristics similar to AATSR, and was originally scheduled for launch in late 2013 aboard the ESA/GMES Sentinel-3A satellite. After several postponements, the Sentinel-3A satellite was carried into orbit on a Rockot launcher from Plesetsk, Russia, on 16 February, 2016.

Although the SLSTR data did not become available during the project, its use for ash retrieval was investigated. SLSTR has characteristics similar to AATSR (*Donlon et al. 2012*), and the ash retrieval methods developed in VAST can be applied to SLSTR data. The differences between the instruments

and the possible effects on aerosol retrieval have been studied. SLSTR has wider swath (1420 km at nadir) than AATSR (500 km), higher resolution (0.5 km) for VIS channels, two additional channels, and a two-satellite configuration (after Sentinel-3B has been launched). Similar to AATSR, it is a dual-view instrument, although the oblique view direction is changed from the forward looking one of AATSR to a backward view in SLSTR. The ash retrieval methods developed for AATSR can be adjusted for use with SLSTR data. The preparatory work on SLSTR is summarized in the EO data report (*Virtanen and de Leeuw, 2015*).

## 4. MODELLING DEVELOPMENT

VAST worked on developing and improving modelling tools used for predicting the transport of volcanic ash and SO<sub>2</sub> in the atmosphere, in particular focusing on incorporating observations into the models in order to obtain more reliable model simulations. The main VAST modelling tools and techniques are

1. **Source term inversion** used for determining the source term of ash and SO<sub>2</sub> during volcanic eruptions, utilizing satellite observations as a constraint.
2. **Data assimilation** used for correcting errors in the transport model and input data by updating the modelled fields with up-to-date observations.
3. **Ensemble modelling** used for inferring uncertainties related to the model simulations arising from the meteorological data driving the model, the source term or inherent in the model itself.
4. **Model inter-comparison and validation:** Within VAST three different atmospheric dispersion models were available and inter-compared for their ability to simulate volcanic ash and SO<sub>2</sub> in the atmosphere. Evaluating model results with real observations is key to understanding their quality and to further improving the modelling tools.

These tools and techniques were applied to several historical eruption case studies for extensive analysis of the tools and the modelling capabilities. Furthermore, a prototype of a dynamic inverse modelling tool, capable of being run in near real-time, was developed within VAST.

### 4.1 Inverse modelling

The VAST-NILU team analysed, together with *Moxnes et al. (2014)*, the separation of volcanic ash and SO<sub>2</sub> from the **Grimsvötn-2011** eruption on Iceland. This was the first time inverse modelling was used to constrain the source terms of SO<sub>2</sub> and ash from the same eruption, based on the work of *Stohl et al. (2011)*. Using IASI satellite data to constrain the source terms, it was found that the SO<sub>2</sub> emissions occurred at an earlier stage and at higher altitudes than the ash emissions (*Figure 4-1*). This led to very different transport patterns, which were successfully simulated by the FLEXPART dispersion model: SO<sub>2</sub> was transported mostly north- and westwards, while ash was transported south- and eastwards (*Figure 4-2*) and crossed Scandinavia at a low altitude where it was measured at ground-based

measurement stations. These measurements, as well as independent satellite data from SCIAMACHY, GOME-2 and CALIPSO, ground-based LIDAR data, and aircraft data, were used to validate the modelled ash and SO<sub>2</sub> clouds. It was found that using the source term constrained by IASI satellite data, the modelled SO<sub>2</sub> and ash clouds were well simulated by the model. During this work the inverse modelling tools were further enhanced and the ability of the inverse modelling system in separating between SO<sub>2</sub> and ash was successfully demonstrated.

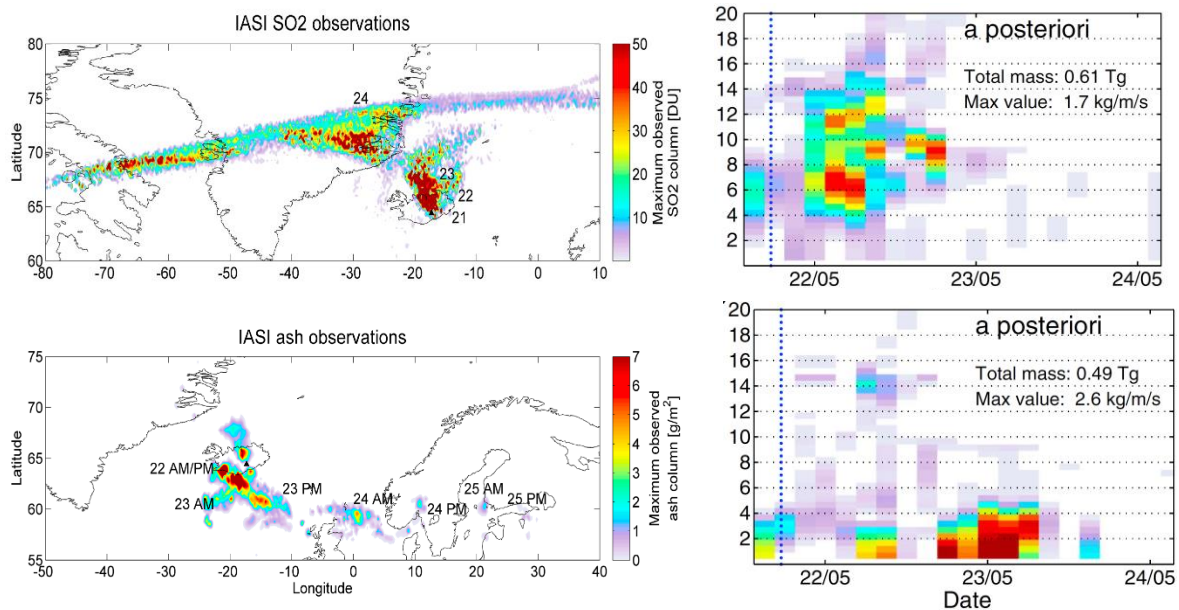


Figure 4-1: IASI satellite observations (left panel) of SO<sub>2</sub> (top) and ash (bottom) of the Grimsvötn-2011 eruption, and the vertically and temporally resolved source terms (right panel) of SO<sub>2</sub> (top) and ash (bottom) determined by inverse modelling. Figures from Moxnes et al. (2014).

The VAST-inverse modelling tools were also applied to the **2014-Kelut eruption** (Indonesia) (Kristiansen et al., 2015). This particular eruption was given attention due to an accidental aircraft encounter, and it was hoped that modelling could provide an estimate of how much ash the aircraft encountered. Satellite ash retrievals from MTSAT observations and FLEXPART transport modelling were combined within the VAST inversion framework to estimate the volcanic ash source term and to study ash transport. For this particular case, both the temporal and horizontal resolutions of the inverse modelling system needed to be increased in order to resolve the source term at the appropriate resolution. The retrieved source term (Figure 4-2) showed that the largest ash emissions occurred at about 16 km altitude where a strong tropopause temperature inversion was found. A total of 0.74 Tg of fine ash was released into the atmosphere according to the estimated source term, with about 51% (0.38 Tg) injected into the stratosphere (above the tropopause at 16.5 km).

Other satellite instruments such as CALIOP, MODIS, AIRS and MLS also imaged the ash plume and provided insights into the size, shape and altitude of the eruption cloud in the atmosphere, which was also used for validation of the source term and modelled ash cloud. CALIOP measured its strongest signal in altitudes around 17-18 km, with the top of the umbrella cloud at 18-19 km (Figure 4-2e). This compares well with the major source term altitudes at around 17 km. Some higher emissions around



22 and 25 km were seen by CALIOP. MODIS plume topography, estimated using single-channel thermal measurements (*Figure 4-2d, inset figure*), suggests plume tops ranging from about 18 km to 26 km. The modelled ash clouds were analysed to estimate the ash concentrations along the flight track of the commercial aircraft that encountered it (*Figure 4-3*). It was demonstrated that, in this particular case, satellite data could not be directly used to observe the ash cloud encountered by the aircraft due to saturation of the satellite-measured signals at the location and time of the encounter, whereas inverse modelling – incorporating also later unsaturated observations - revealed its presence during the encounter. This shows that the combination of satellite observations and modelling is the key to obtaining a robust evaluation of this event.

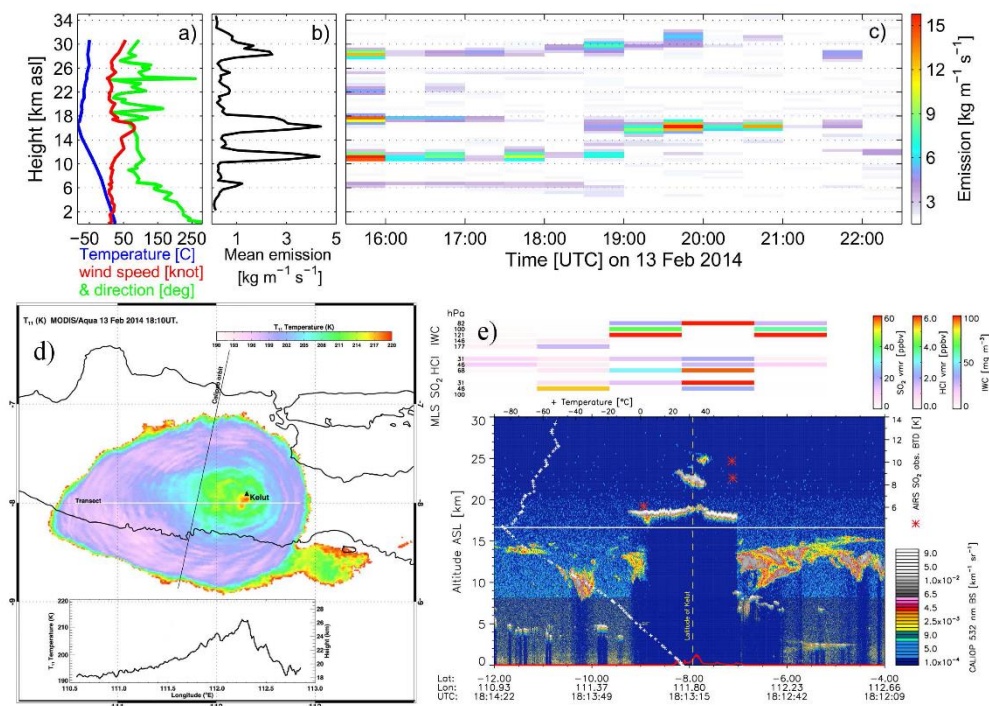


Figure 4-2: Kelut-2014 source term and meteorological observations (a,b,c), MODIS satellite observations (d), and MLS and CALIOP measurements (e). Figure from Kristiansen et al. (2015).

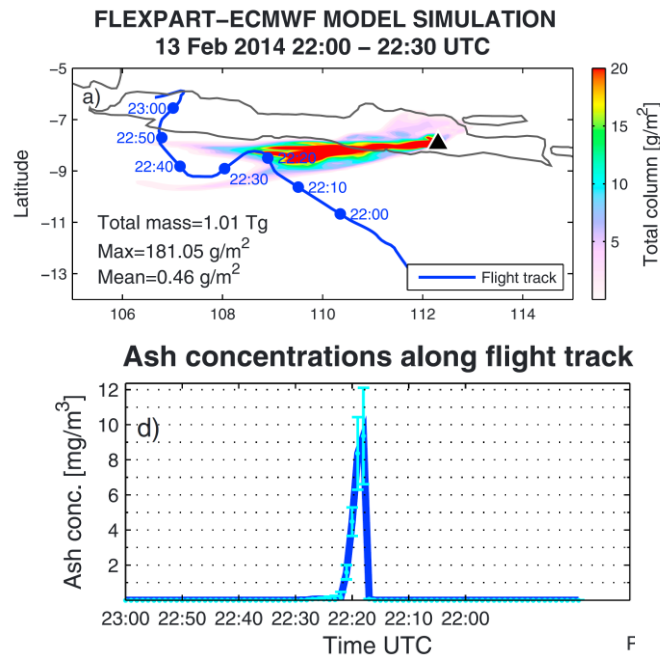


Figure 4-3: Kelut-2014 modelled ash cloud (top) overlaid with the flight track of the aircraft that encountered the ash cloud (blue line). Modelled ash concentrations along the flight track (bottom). Figure from Kristiansen et al. (2015).

## 4.2 Data assimilation

The VAST-FMI team has developed and tested inverse modelling and data assimilation techniques, in order to understand ways to improve the accuracy of the model forecasts. Analyses of these techniques were done for the SO<sub>2</sub> cloud from the Grimsvötn-2011 eruption based on the SILAM dispersion model equipped with variational methods represented by 4D-VAR. These procedures are also suitable for automated volcanic SO<sub>2</sub> source inversion and plume forecasting, and can be suitable also for volcanic ash.

Comparison of the approaches revealed noticeable differences in their features and performances. In particular, the 4D-VAR data assimilation following the classical procedure (direct assimilation of downwind satellite observations without considering the source term) showed the best agreement with the assimilated satellite data, but proved to provide a quite weak basis for the forecasts.

The main difference between the source term-inversion and data-assimilation procedures is shown in Figure 4-4. The inversion accumulates the information for each day since the start of the eruption into an extending assimilation window. This information is used to identify temporal evolution of the source emission, which is then used for the forecasting. The standard data assimilation-based analysis is performed for each day individually providing the daily observation patterns. The last-day pattern is used for the forecasting without any source term defined.

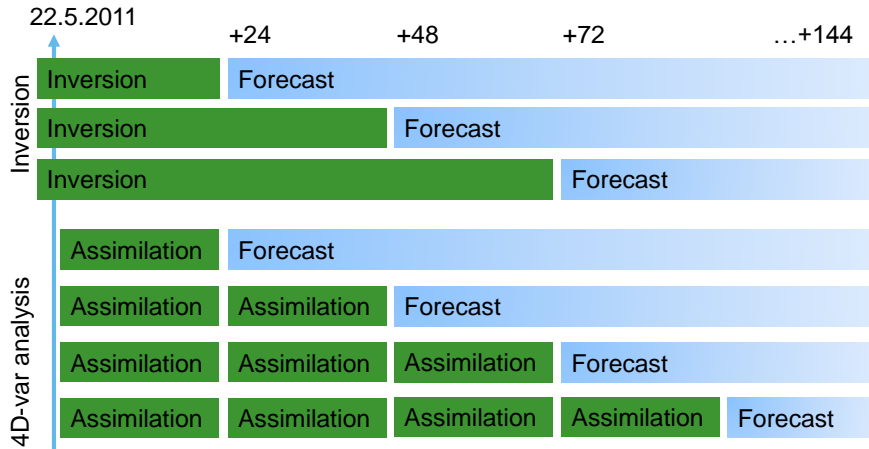


Figure 4-4: Steps of source inversion and assimilation analysis procedures

The difference between these two approaches and the effect on the model forecasts is quite substantial, as seen in Figure 4-5. Both approaches showed similar location of the main mass over Greenland, but analysis from the data assimilation showed significantly larger affected areas than the simulations from the inversion.

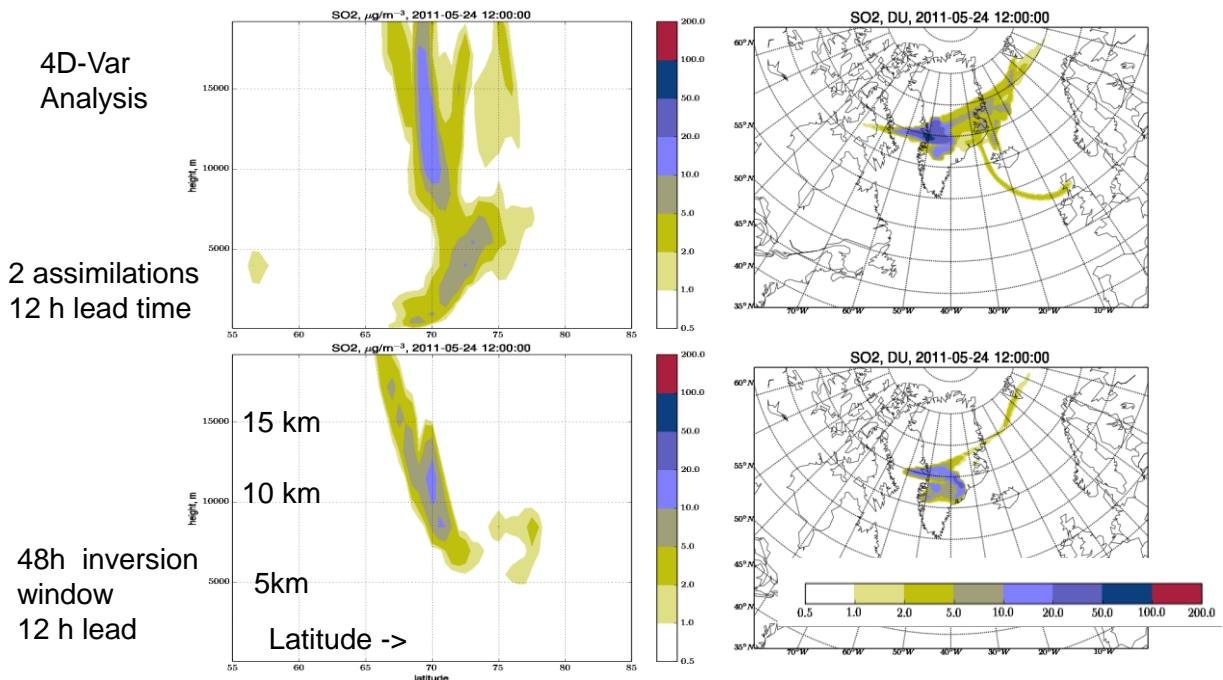
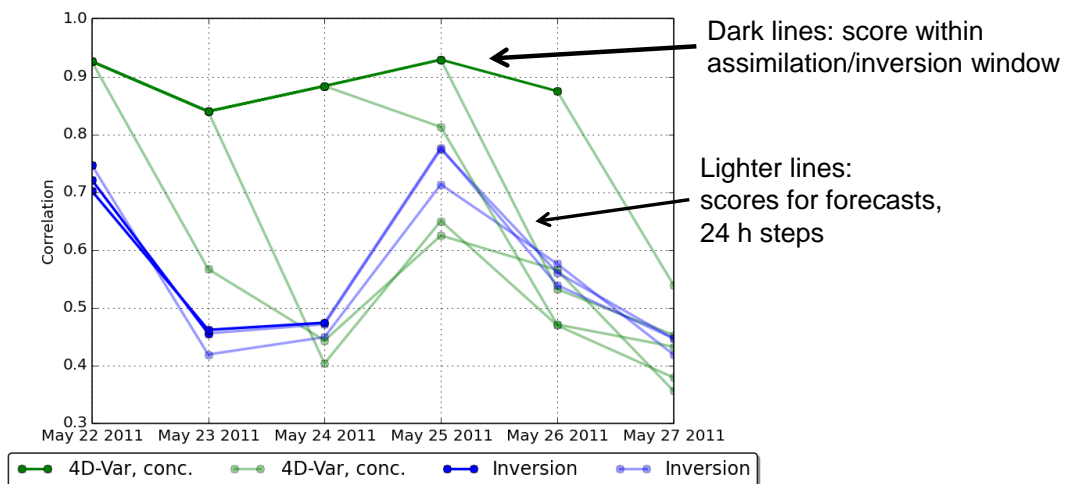


Figure 4-5: Comparison of the total columns and zonal means of  $SO_2$  concentrations from the Grimsvötn eruption, 24 May 2011 at 12:00, applying two different approaches: 4D-Var data assimilation (top row) and source term inversion (bottom row).

The comparison between the SO<sub>2</sub> data assimilation and inversion approaches with OMI is illustrated in *Figure 4-6*. The evolution of a series of assimilations (dark green lines), inversions (blue lines) and the corresponding forecasts (light lines) is shown. The best agreement with OMI is obtained with the classical data assimilation, which uses the same OMI retrievals for determining the plume position and evolution during each specific day (dark green line). It significantly outperforms the inversion-based approach (dark blue line), which is constrained at the volcano location. The situation, however, changes when the forecasts are considered. The model predictions initialized from the assimilation analysis deteriorate immediately and fall below the inversion-driven predictions. The quality of the inversion-driven forecasts and analyses are essentially the same, i.e. that approach appeared much more robust than the data assimilation.

The main reason for the low quality of the assimilation-driven forecasts is that the column-integrated retrievals provide insufficient information to constrain the plume vertically. This results in quick deterioration of its shape when the unconstrained forecast is run. Accumulation of the information through several days and, most importantly, fixed location of the volcano as the only source of the observed plumes appears important for reliable forecasts. Application of very long inversion windows does not bring much improvement since observations far from the source are not efficient constraints for the source and the forecasted plume. Also incomplete coverage of the plume by each specific overpass of OMI - some areas remain non-observed - is a challenge for the assimilation.



*Figure 4-6: Spatial correlation coefficient between daily patterns observed by OMI and simulated by SILAM using the source inversion (blue lines) and standard assimilation (green lines)*

### 4.3 Ensemble modelling

Ensemble modelling has been a key part in VAST. The VAST-FMI team developed and tested ensemble Kalman filter (EnKF) techniques based on the SILAM dispersion model, which was tested for the Grimsvötn-2011 SO<sub>2</sub> eruption cloud. Also, VAST-ZAMG developed an ensemble-modelling approach based on the FLEXPART model using ECMWF-ensemble members to perform multiple model

simulations taking into account the uncertainty in the meteorological data driving the dispersion model. These procedures are also suitable for automated plume forecasting.

### 4.3.1 Ensemble Kalman Filter as a source inversion technology

The aim with the EnKF was to construct an assimilation scheme where an ensemble would provide an envelope for the possible plume locations. A mirroring concept was applied where the envelope was assumed and stayed in the ensemble until excluded by the observations. The “assumed” and “confirmed” plumes could be distinguished by the ensemble spread.

The SILAM model has recently been equipped with Ensemble Kalman Filter technology (TOPAZ EnKF code), which was applied to volcano source term inversions. The aim of the experiment was to construct an assimilation scheme, where the ensemble would provide an envelope for the possible plume locations. Construction of the EnKF-based inversion required perturbation of the volcanic source term, which would keep its location but involve some stochastic description of the emission intensity and vertical injection profile. A total of 80 ensemble members was calculated, and OMI data was used for constraining the obtained plumes.

The ensemble identified very complicated vertical structures of the plume (*Figure 4-7*) and their reliability is marked by the ensemble standard deviation. A very thick vertical column is suggested for 23 May 2011 (upper row of *Figure 4-7*) but this is, in fact, very uncertain, as shown by the ensemble standard deviation exceeding the mean value. Conversely, the 8-km cloud containing the bulk of the plume mass is quite well-defined: its standard deviation is lower than the mean value. With time, increasing amount of observations and longer plume development allow for more definite constraining of the plume: by 27 May 2011 practically all parts of the vertical plume structures are well-defined.

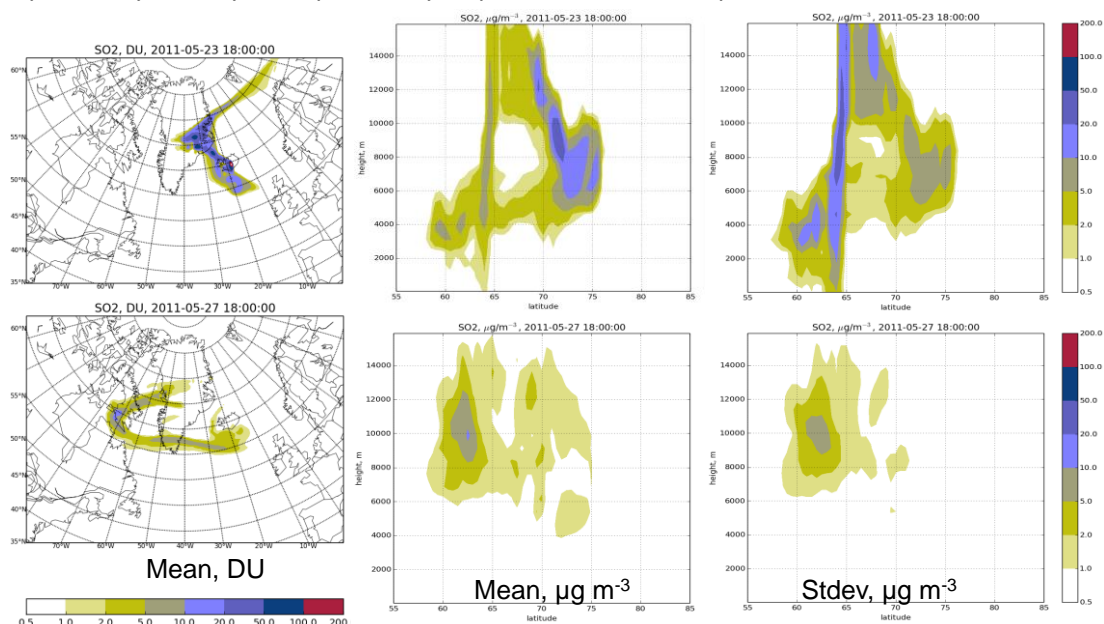
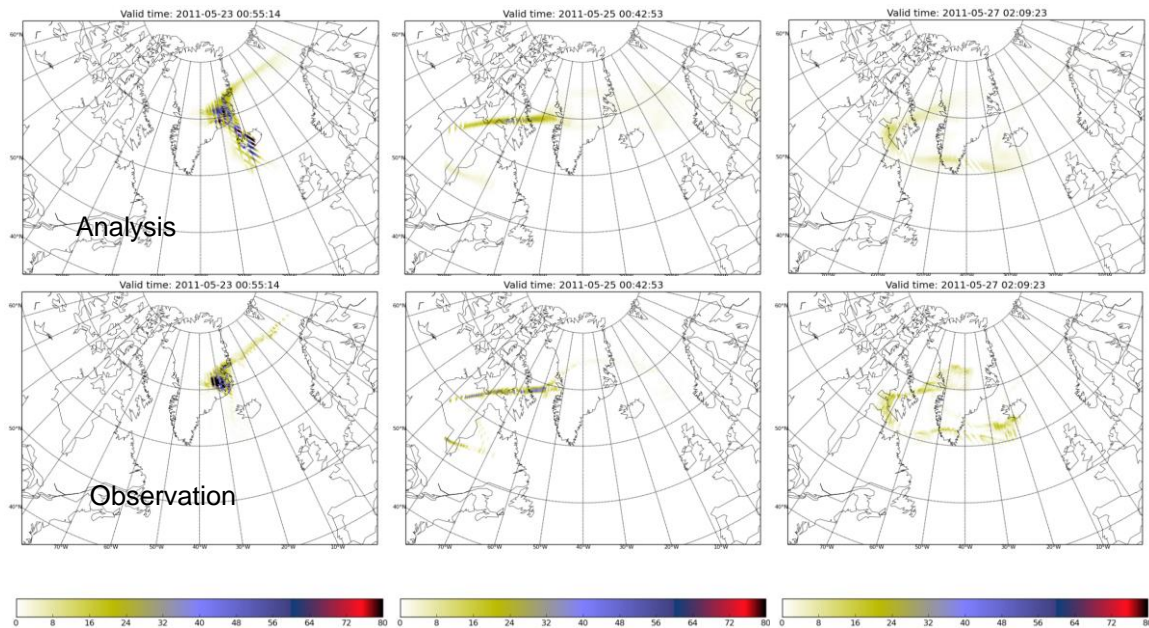


Figure 4-7: EnKF simulations: the column-integrated plume, zonal average, and its ensemble standard deviation, for two days: 23 and 27 May 2011 (third and seventh days of the Grimsvötn eruption).

The quality of the EnKF analysis is confirmed by its comparison with OMI observations (*Figure 4-8*). At the early stages the uncertainty is larger and the ensemble is capable of capturing only the major plume location and its tail toward north-east. These main features are reproduced quite accurately but the plume connection with source in Iceland is quite unclear. With time passing, the analysis improves and reaches very good agreement already by 25 May 2011.



*Figure 4-8: Comparison of EnKF analysis (upper row) with OMI satellite observations (bottom row) for 23, 25 and 27 May 2011 of the Grimsvötn eruption.*

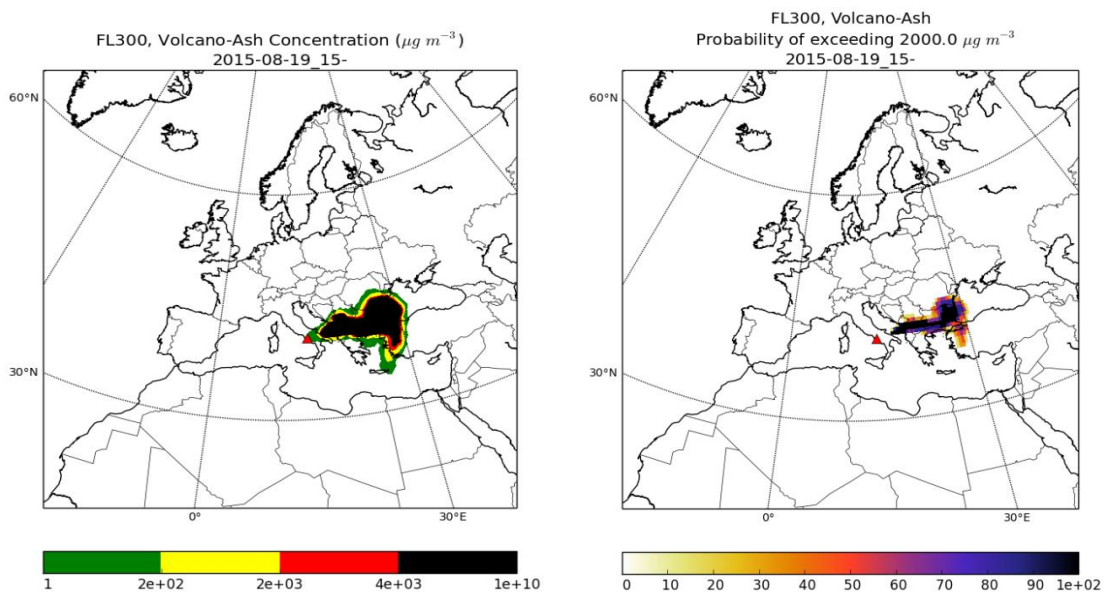
#### 4.3.2 Multi-input ensemble using ECMWF meteorological ensembles

Multi-input ensemble modelling is a pragmatic approach to account for the uncertainties associated with the meteorological driving data, whereby several atmospheric transport model calculations are performed using different, but equally probable, meteorological data sets from one forecasting system. The European Centre for Medium-Range Weather Forecasts (ECMWF) Ensemble Prediction System (ENS) is a useful data source for ensemble studies (*Galmarini et al. 2010*) dealing with the uncertainty of the medium-range weather forecast. It consists of 50 equally probable forecasts originating from different perturbations of the initial state. The master thesis performed within the VAST framework by *Klonner (2013)* investigated in detail the potential implementation of such an approach into an operational environment for volcanic ash forecast. The limited resources and time requirements constraining an operational system prevent using the full set of 50 members to perform 50 volcanic ash forecasts with FLEXPART, followed by the generation of comprehensive ensemble products. Therefore a solution must be obtained that keeps the usefulness of an ensemble approach with a smaller number of ensemble forecasts to be carried out. *Klonner (2013)* investigated the possibility of performing a pre-selection of a sub-set of the 50 ENS members by clustering the

horizontal wind ( $u, v$ ) components of one model level (around 8 km) that is significant for aviation purposes and for the region where the plume is expected. This implies that the clustering can only be applied in case of high-altitude eruptions (greater than 8 km a.g.l.). Once the representative ENS members (around 5) are identified, the meteorological data are retrieved and used to drive the various FLEXPART ensemble member forecasts and produce the ensemble products.

This approach has been implemented in the operational demonstration service at ZAMG. The multi-input ensemble products consist of the 'standard' output for the operational forecasts (e.g. total column loading, concentrations at various flight levels, vertical cross sections at specific locations etc., for details see Section 8.1) together with the maximum concentrations and Agreement in Threshold Levels (ATL) of the representative ensemble forecasts plus the 'standard' operational forecast (maps and time-height cross sections). An example is shown in *Figure 4-9*.

Although the clustering performed before retrieving the meteorological data and performing the FLEXPART calculations reduces the time needed to perform the multi-input ensemble modelling substantially, computing time is still hindering its full capabilities. The user will first obtain the operational forecast and, after 12 hours, the ensemble products will be available.



*Figure 4-9: Maximum concentration (left panel) and ATL plot (right panel) for FL 300 combining forecasts with operational meteorological input and input from selected ensemble members.*

## 4.4 Model inter-comparison

The VAST-NUIG team further developed the WRF-Chem model for simulations of volcanic ash. In particular the WRF-Chem model was optimised in terms of boundary layer parameterisation, convection schemes and microphysics schemes for volcanic ash events. In addition, a semi-automated process for volcanic ash forecasting was developed. Further, the model was developed for the possibility to run on time and height dependent volcanic ash fluxes based on the FLEXPART source term inversion results. This allowed to harmonise the source term for validation purposes using historical eruptions as test cases to quantify variability between model outputs. The contribution of individual ash loss mechanisms was also quantified.

The entire VAST modelling team (NILU, ZAMG, FMI and NUIG) joined in a model-inter-comparison effort (Kristiansen *et al.*, 2015), studying the Grimsvötn-2011 eruption. The team simulated the dispersion of ash from the eruption, with three different dispersion models (FLEXPART, SILAM and WRF-Chem), all using the same ash source term as derived by Moxnes *et al.* (2014), and the same meteorological input data to the models. The aim with the model inter-comparison and model mini-ensemble was to investigate how well the models could simulate the ash clouds (compared to real observations, Figure 4-11), and also how the three models differed in terms of ash cloud extent and ash amounts (Figure 4-10). The differences that occurred between the three models would be due to the models' formulations of physical processes such as loss mechanisms (wet deposition, dry deposition, sedimentation) and associated with on-line (WRF-Chem) and off-line (SILAM and FLEXPART) meteorology. Very good agreements were found between the SILAM and FLEXPART models, while WRF-Chem systematically showed ash clouds with larger horizontal extents, and therefore larger total amount of ash in the atmosphere than the two other models (Figure 4-10 and Figure 4-11). This points towards differences in the loss mechanisms and handling of meteorological data between WRF-Chem and the two other models, however more work is needed in order to fully understand the details of the underlying causes of the differences between the models.

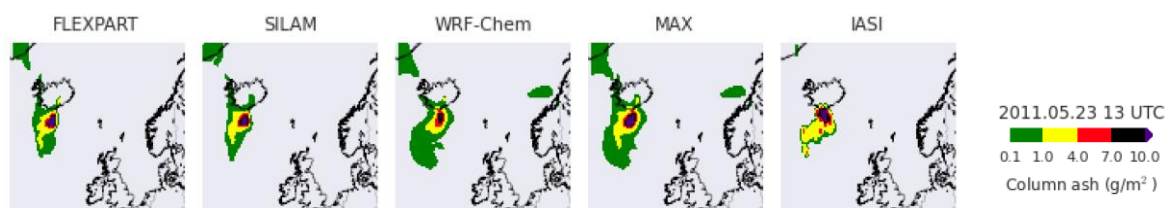


Figure 4-10: Grimsvotn-2011 modelled ash cloud simulated by three different transport models: FLEXPART, SILAM and WRF-Chem using the same ash source term from Moxnes *et al.* (2014) (Figure 4-1) and based on the same meteorological input data to the models. The maximum column loading between three models are also shown, as well as IASI satellite observations.



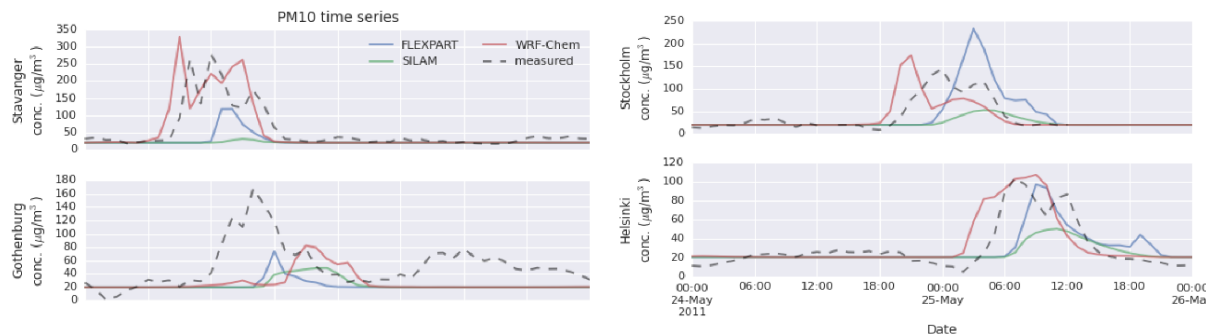


Figure 4-11: Grimsvotn-2011 modelled ash cloud simulated by three different transport models (FLEXPART, SILAM and WRF-Chem) compared to ground-based PM10-measurements at different stations in Scandinavia.

## 5. VALIDATION AND INTERCOMPARISON

A main tasks of VAST was the validation of EO and modelling products. While validation efforts were carried out within each task separately, a designated validation work package focused on an independent validation of specific VAST products. Results of this work are given in the Product Validation Report (O'Dowd, 2016). As an example below the validation of results from the FLEXPART off-line dispersion model, used as the primary VAST ash cloud forecasting model, is shown. AATSR, onboard the polar orbiting ENVISAT satellite, was used to evaluate the ash column mass and plume height.

FLEXPART forecasts for the Eyjafjallajökull eruption, driven with a source-term constrained by ash mass loading retrievals from SEVIRI data, were compared to ash mass loadings quantified from AATSR data. The comparison showed that the mass loadings from AATSR retrievals were much higher than the column ash mass modelled by FLEXPART, with the modelled mean value being a factor of 2.4 to 6.8 times lower than that quantified by AATSR. This difference is mainly due to the fact that the TIR and VIS/NIR methods are sensitive to different particle sizes, and FLEXPART was driven with a source term constrained by SEVIRI TIR data. Further, plume heights modelled by FLEXPART were compared with AATSR-observed plume heights, and showed good match, particularly close to the volcano (Figure 5-1); however, as distance increased from the source, the agreement with the modelled plume height deteriorated notably.

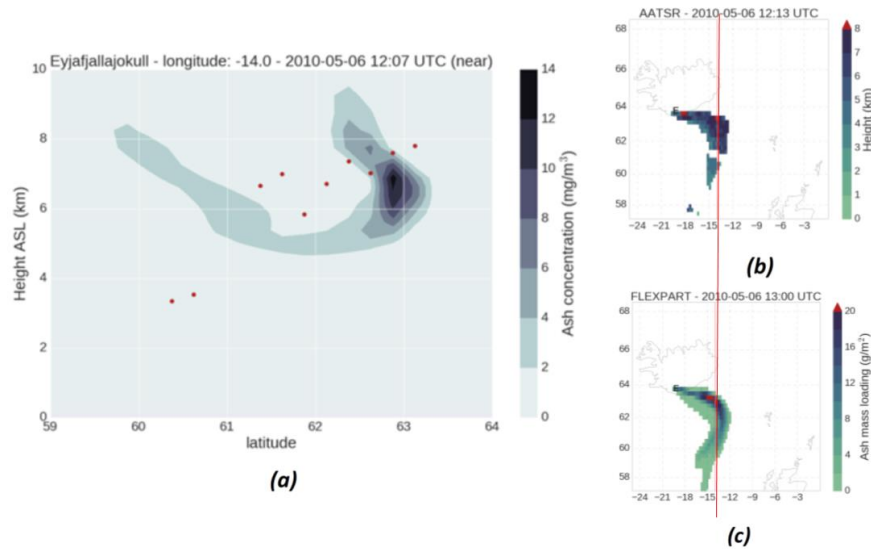


Figure 5-1: AATSR top ash plume heights (red circles) superimposed over FLEXPART ash concentrations for the near eruption location (a). AATSR height and c) FLEXPART ash mass loading with the position of transect marked by a red line (b).

Furthermore, validation efforts were made during both the ESA funded project SAVAA (Support to Aviation for Volcanic Ash Avoidance; 2009-2012) and VAST. Several case studies were performed (see e. g. *Stohl et al., 2011; Kristiansen et al., 2012; Moxnes et al., 2014*) which focussed on evaluating the observational and modelling capacities of volcanic ash and SO<sub>2</sub> clouds, including extensive validation using independent measurement data.

*Stohl et al. (2011)* and *Kristiansen et al. (2012)* analysed the ash clouds from the 2010-Eyjafjallajökull eruption, while *Moxnes et al. (2014)* analysed the ash and SO<sub>2</sub> clouds from the 2011-Grimsvötn eruption. One of the keys for achieving more reliable model simulations of volcanic eruption clouds is incorporating observation data into the models. Inverse modelling was used in all cases to calculate the a posteriori source term, constrained by satellite observations. Model simulations using the a posteriori source term were compared to model simulations using a simpler a priori source term not constrained by satellite data. The model simulations were evaluated using ground based observations such as web cameras, LIDAR, and particulate matter measurements, as well as spaced based LIDAR observations of the eruption column, and aircraft observations. It was found that the inversion consistently improved the quality of the model simulation for all case studies.

The a posteriori simulations showed better skill when compared statistically to the observations than the simulations using the simpler a priori source term. The improved agreement with the observations comes from the more accurate a posteriori plume positions and concentration levels. For example, an increase in the correlation between observed and measured ash concentrations from -0.02 (a priori) to a significant moderate positive correlation 0.36 for the a posteriori simulation was obtained for the Eyjafjallajökull ash cloud (*Figure 5-2*). For the 2011-Grimsvötn eruption, model simulations with the satellite-constrained a posteriori source term were able to successfully simulate the separation of the

SO<sub>2</sub> and ash with the SO<sub>2</sub> first moving north- and then westward and most of the ash first moving south- and then eastward. Transport simulations using a simpler a priori source term with a uniform vertical distribution were not able to capture this separation.

Overall, the consistent improvements in the a posteriori simulations over the a priori simulations demonstrate that the inversion provides invaluable information that, on a near-real time basis, should be used as input to the dispersion models. This will give more accurate representations of the transport of volcanic eruption clouds and increase the accuracy in volcanic ash forecasts.

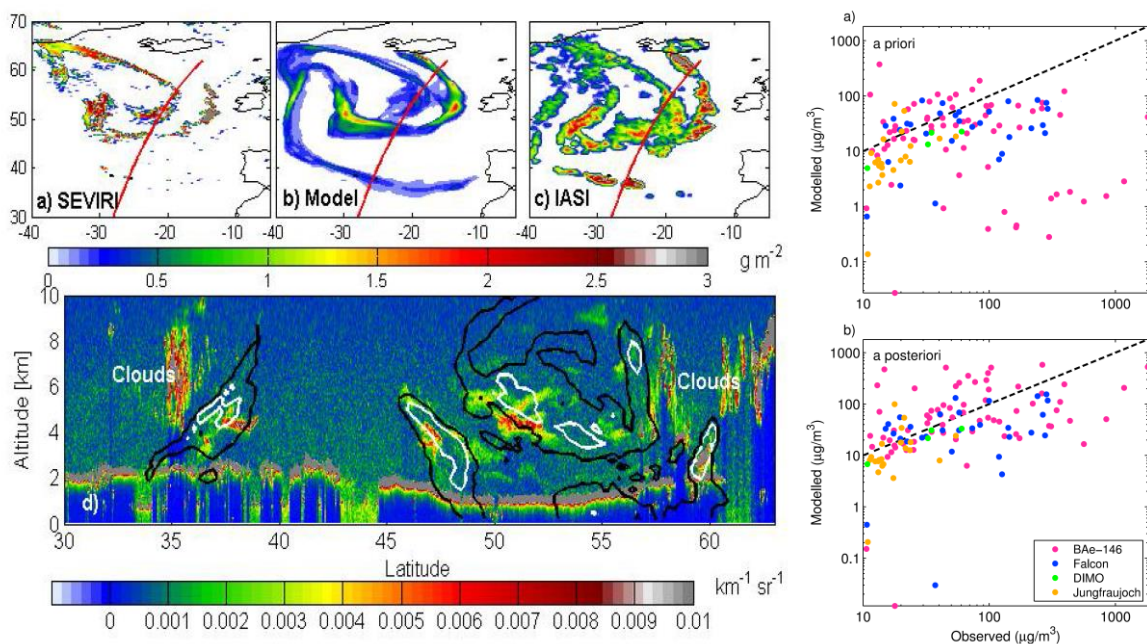


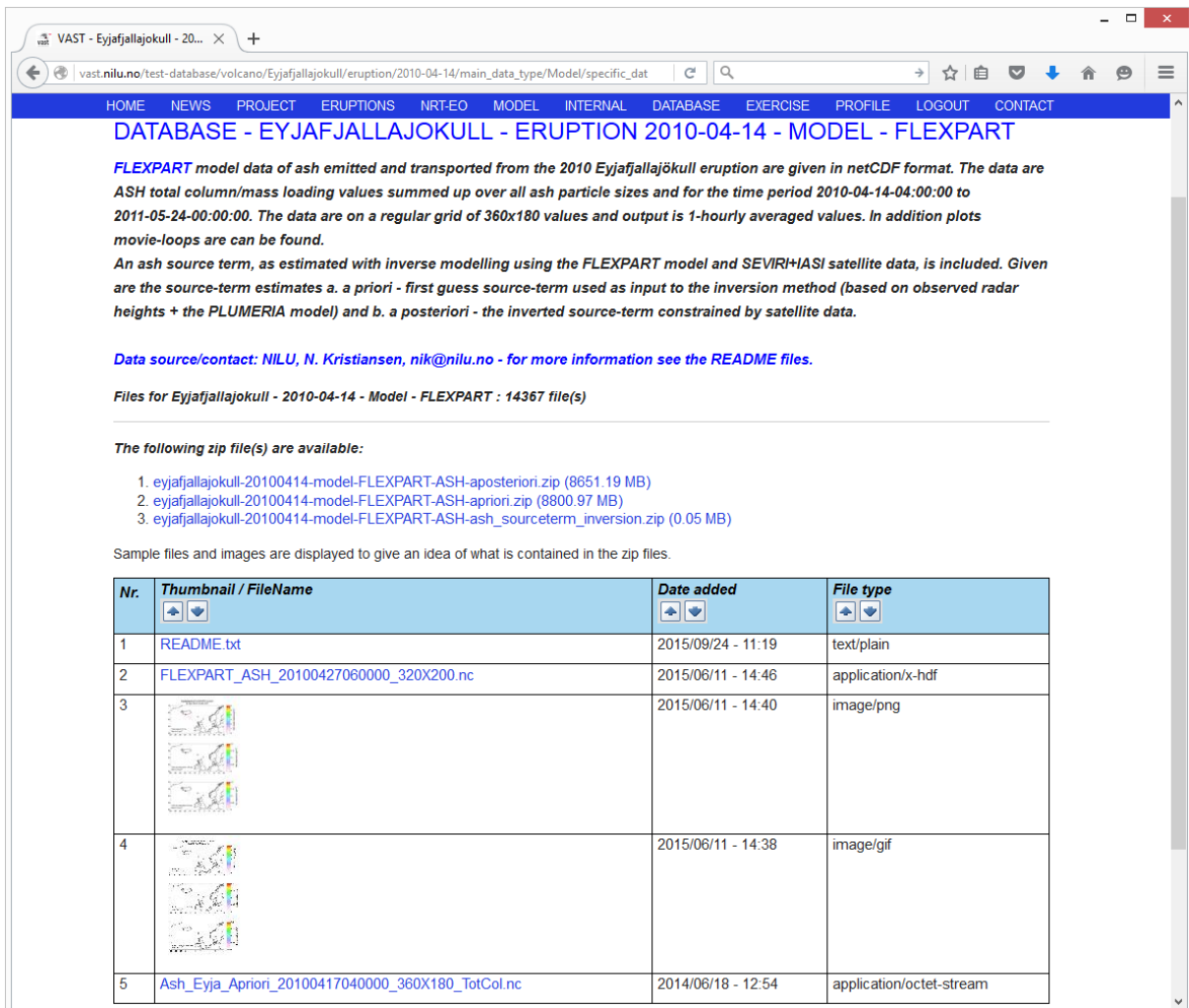
Figure 5-2: Right: Validation of a posteriori model simulations with satellite observations (SEVIRI, IASI and CALIOP) on 10 May 2010. The lower left figure shows the CALIOP vertical cross-section along the red line shown in (a–c) of total attenuated backscatter at a wavelength of 532nm (coloured) superimposed with 20  $\mu\text{g m}^{-3}$  (black line) and 200  $\mu\text{g m}^{-3}$  (white line) volcanic ash concentrations from the a posteriori model simulation. From Figure 7 from Stohl et al. (2011). Left: Illustration of improved a posteriori model simulations by validation with aircraft and ground-based measured ash. The Pearson's correlation coefficients (PCC) are -0.02 (a priori simulation, top) and 0.36 (a posteriori simulation, bottom). From Figure 16 of Kristiansen et al. (2012).

## 6. DATABASE FOR HISTORICAL ERUPTIONS

As a response to the requirement “R1 Access to all data sources of volcanic plume observations in Europe should be accelerated, improved and open” from *Zehner (2012)*, the VAST team compiled a benchmark test dataset for seven historic volcanic eruptions.

The VAST, the SACS-II (Support for Aviation Control Service), the SMASH (Study on an end-to-end System for volcanic ASH plume monitoring and prediction) teams, individual researchers, as well as research networks provided datasets (data originators are specified in readme files in the database). The database contains satellite, model and *in situ* data from the following eruptions: Eyjafjallajökull, Iceland (April-May 2010), Grímsvötn, Iceland (May 2011), Kasatochi, Alaska, USA (August-September 2008), Etna, Italy (various dates, 2011), Puyehue-Cordón Caulle, Chile (June 2011), Chaitén, Chile (May 2008), and Mount Kelut, Indonesia (February 2014).

The database is accessible via the [vast.nilu.no](http://vast.nilu.no) website for registered users. For a description of the content see *Stebel et al. (2015)*. An example database page is shown in *Figure 6-1*. Users have to accept the data usage protocol, protecting the data ownership rights of the data provider. Users can then search and download the results, data, plots, and readme files, as a compressed archive (zip). More details of the individual data sets are given in the respective readme files and thumbnail/example images files are added as illustration.



VAST - Eyjafjallajökull - 20... x

vast.nilu.no/test-database/volcano/Eyjafjallajökull/eruption/2010-04-14/main\_data\_type/Model/specific\_dat

HOME NEWS PROJECT ERUPTIONS NRT-EO MODEL INTERNAL DATABASE EXERCISE PROFILE LOGOUT CONTACT

## DATABASE - EYJAFJALLAJÖKULL - ERUPTION 2010-04-14 - MODEL - FLEXPART

**FLEXPART** model data of ash emitted and transported from the 2010 Eyjafjallajökull eruption are given in netCDF format. The data are ASH total column/mass loading values summed up over all ash particle sizes and for the time period 2010-04-14-04:00:00 to 2011-05-24-00:00:00. The data are on a regular grid of 360x180 values and output is 1-hourly averaged values. In addition plots movie-loops are can be found.

An ash source term, as estimated with inverse modelling using the FLEXPART model and SEVIRI+IASI satellite data, is included. Given are the source-term estimates a. a priori - first guess source-term used as input to the inversion method (based on observed radar heights + the PLUMERIA model) and b. a posteriori - the inverted source-term constrained by satellite data.

**Data source/contact:** NILU, N. Kristiansen, [nik@nilu.no](mailto:nik@nilu.no) - for more information see the README files.

Files for Eyjafjallajökull - 2010-04-14 - Model - FLEXPART : 14367 file(s)

The following zip file(s) are available:

- eyjafjallajökull-20100414-model-FLEXPART-ASH-aposteriori.zip (8651.19 MB)
- eyjafjallajökull-20100414-model-FLEXPART-ASH-apriori.zip (8800.97 MB)
- eyjafjallajökull-20100414-model-FLEXPART-ASH-ash\_sourceterm\_inversion.zip (0.05 MB)

Sample files and images are displayed to give an idea of what is contained in the zip files.

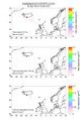
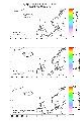
Nr.	Thumbnail / FileName	Date added	File type
1	README.txt	2015/09/24 - 11:19	text/plain
2	FLEXPART_ASH_20100427060000_320X200.nc	2015/06/11 - 14:46	application/x-hdf
3		2015/06/11 - 14:40	image/png
4		2015/06/11 - 14:38	image/gif
5	Ash_Eyja_Apriori_20100417040000_360X180_TotCol.nc	2014/06/18 - 12:54	application/octet-stream

Figure 6-1: Example of database page: FLEXPART model results for Eyjafjallajökull, Iceland (April-May 2010).

## 7. DOCUMENTATION AND DATA ACCESS

### 7.1 Project webpage

A project website (<http://vast.nilu.no>, see *Figure 7-1*) including internal tools for data distribution and visualisation was set up. The website is based on the Python-based web development framework Django and its related content management system Django-CMS.

The VAST webpage contains a publicly available part including final VAST deliverables (see <http://vast.nilu.no/project/deliverables/>), results, dissemination and information on recent eruptions (including images of model forecasts). There are also some restricted sections (requires log-in), one with project-specific internal documentation only available to the project members, and one containing an extensive database containing data on volcanic ash available for download to any registered user.

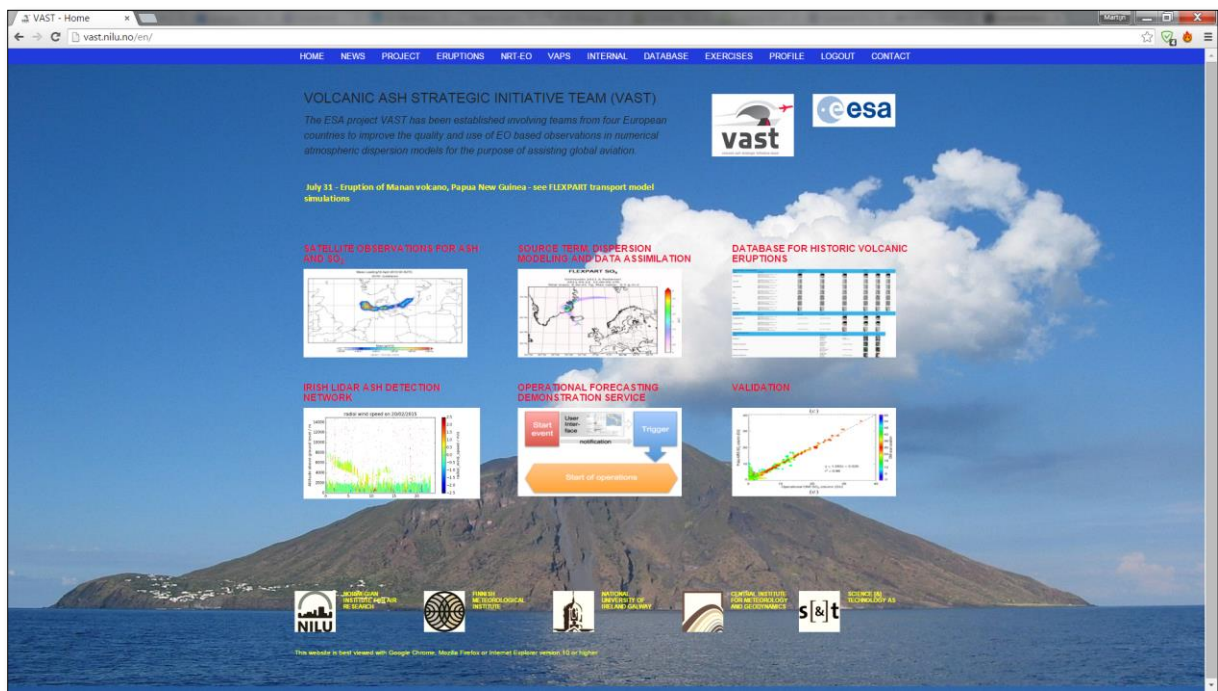


Figure 7-1: VAST project website (main page).

### 7.2 NRT satellite based ash detection, SO<sub>2</sub>, and model results

SEVIRI data are received every 15 min from the NILU EUMETCast receiver. Radiances are converted to brightness temperatures, and pixels are classified according to the new CID ash detection scheme (see *Chapter 3.1*). NRT data and images are shown at <http://fred.nilu.no/sat/>. Examples of available data from the Eyjafjallaökull eruption on May 8, 2010, are given in *Figure 7-2*.

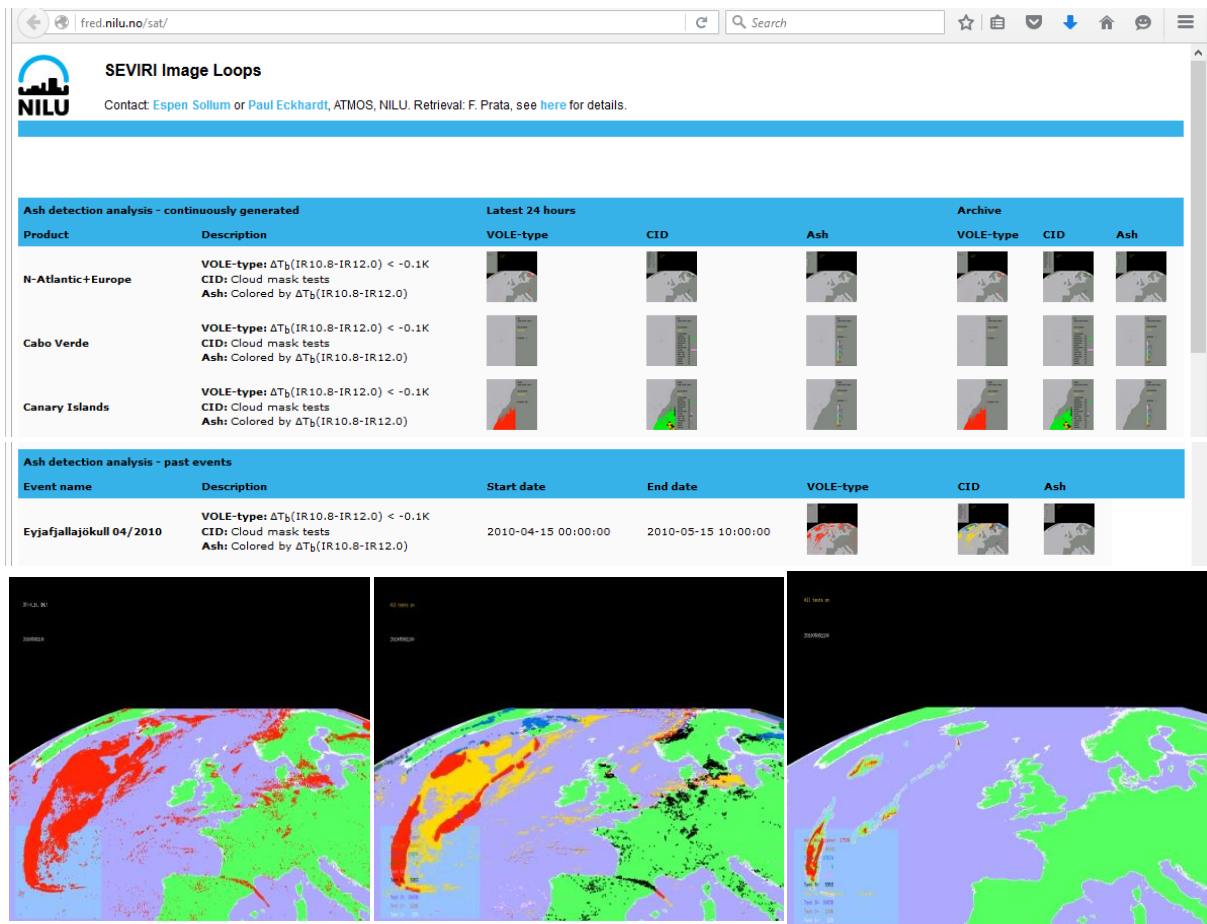
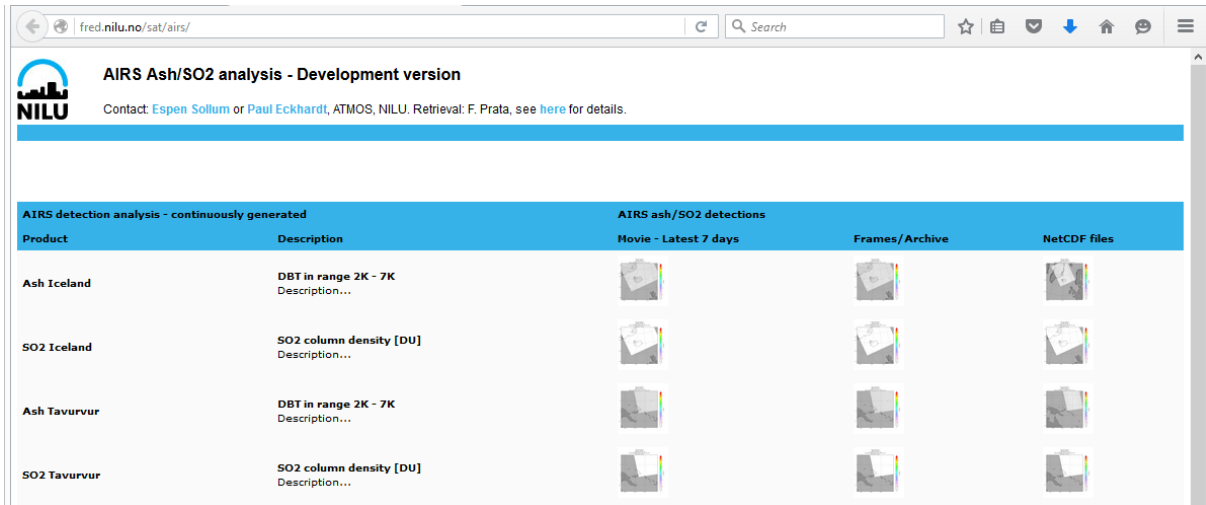


Figure 7-2: NRT SEVIRI ash detection analysis using new CID scheme (Upper panels: Website with access to NRT and historic datasets, Lower panel: Left: Vole-type detection, Middle: CID-detection, Right: Ash detection) Example from May 8, 2010.

NRT and archived ash detection results from AIRS can be found at <http://fred.nilu.no/sat/airs/> (see Chapter 3.2 for a description of the retrieval). Data as well as images can be viewed and downloaded (Figure 7-3). In addition, results from the AIRS SO<sub>2</sub> retrieval, developed in the SAVAA project (see Prata and Corradini, 2009; Prata and Bernardo, 2007) are made available via this website.



The screenshot shows a web browser window with the URL `fred.nilu.no/sat/airs/`. The page title is "AIRS Ash/SO2 analysis - Development version". Below the title, there is contact information: "Contact: Espen Sollum or Paul Eckhardt, ATMOS, NILU. Retrieval: F. Prata, see [here](#) for details." The main content area features a table with the following structure:

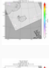
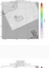
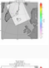

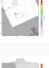

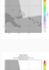
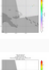
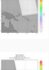



AIRS detection analysis - continuously generated		AIRS ash/SO2 detections		
Product	Description	Movie - Latest 7 days	Frames/Archive	NetCDF files
Ash Iceland	DBT in range 2K - 7K Description...			
SO2 Iceland	SO2 column density [DU] Description...			
Ash Tavurvur	DBT in range 2K - 7K Description...			
SO2 Tavurvur	SO2 column density [DU] Description...			

Figure 7-3: NRT and archived AIRS SO<sub>2</sub> retrieval and ash detection for selected areas.

The model result part of the webpage is described in more detail in **Chapter 8.2 Operational ensemble modelling service**.

- The model results part of the website is a mirror of a ZAMG website, data automatically transferred to NILU from ZAMG.
- Script running every hour fetches the latest results from ZAMG and stores them in the NILU website database.
- The main results page shows the 10 latest operational model forecasts, which can be different from the publicly available list (not all results visible) to the project internally visible list (all results visible) [see **Error! Reference source not found.**].



## 8. OPERATIONAL DEMONSTRATION SERVICE

One of the key parts of VAST was to integrate the developed models and methods into an operational demonstration service at the National Meteorological Center Vienna (ZAMG). The operational integration comprise of the integration of a modelling service, an ensemble modelling service, an ash source term estimating service and various post-processing and graphical tools. The operational demonstration service runs continuously for European significant (ash emissions) events.

### 8.1 Operational model forecasting service

Within VAST a demonstration of an operational forecasting system was developed which produces timely (within the hour) forecast products. The service consists of four components:

**1. Notification system.** The warning system is based on a set of python scripts that gather informative emails from different sources (especially SACS and the VAACs) and produces a digested warning message under a set of user-defined conditions. The most important condition is that a VAAC warning includes a red code for a specific volcano. In addition, messages from the SACS system (<http://sacs.aeronomie.be/>) and the SEVIRI CID and AIRS ash detection ("NILU") are included. Emails with the digested information is sent out to registered users.

**2. Volcano database and related information.** The database includes basic information on all active volcanoes worldwide and default information to obtain the eruption parameters (eruption height and length, fine ash fraction) based on *Mastin et al. (2009)*.

**3. Atmospheric transport model, including a multi-input ensemble modelling option** (i.e. performing atmospheric transport modelling with the same source term, but with different meteorological input). The system arranges the eruption information and the incoming meteorological data to produce forecasts of the atmospheric transport and dispersion of the volcanic fine ash and SO<sub>2</sub>.

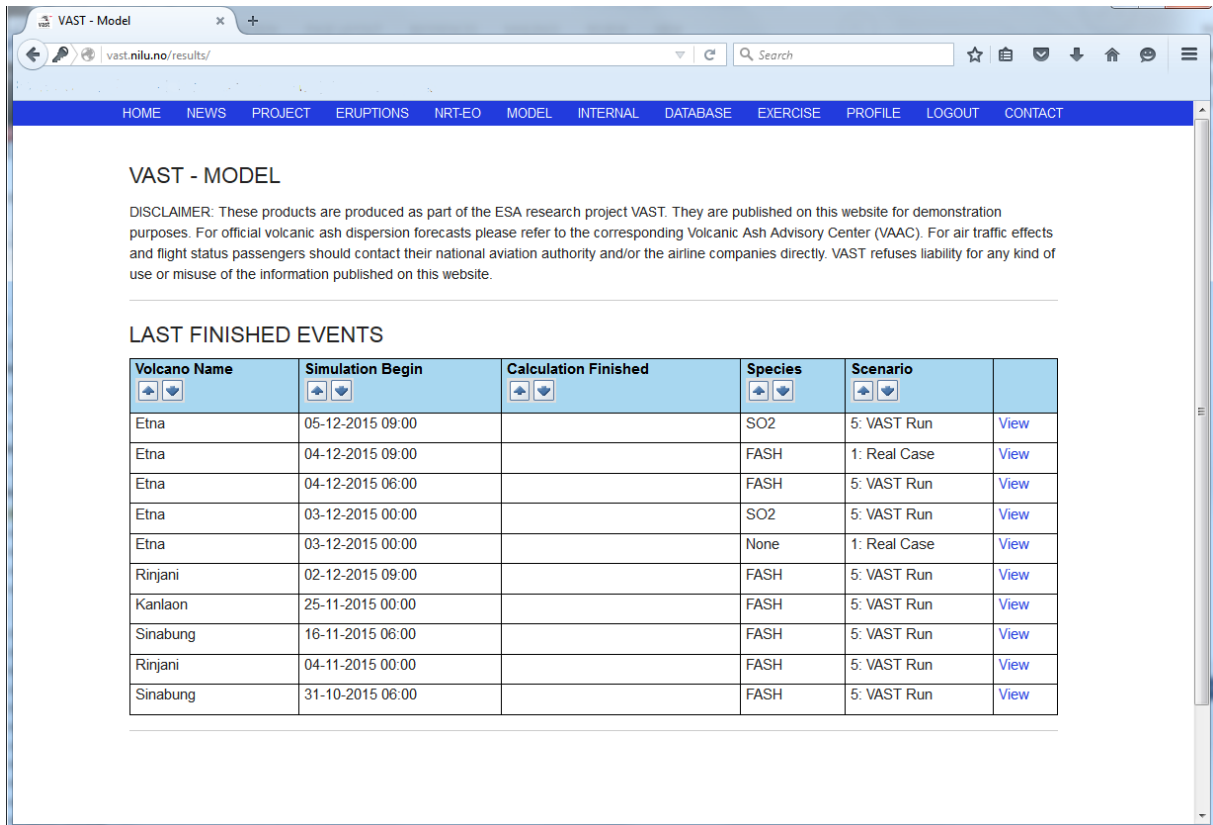
**4. Post-processing.** After the atmospheric transport calculations are finalized, the output is processed to produce maps, cross-sections, and a variety of information depending on the set-up. This includes ensemble products.

The system operates on a continuous basis for significant volcanic eruptions affecting the European air space and on a best-effort basis for worldwide events.

The FLEXPART model output data files are automatically transferred to NILU for relevant cases, including an explanatory readme-file with the specifications of the forecast. In addition, data are automatically transferred to S[&]T to deliver forecasts for a mobile app.

Besides volcanic ash, products for SO<sub>2</sub> - including daily averaged total columns in DU - are available. Multiple releases allow for more complex source terms if needed. Ensemble products, consisting of maximum concentrations and ATL (Agreement in Threshold Level) are also provided if selected.

ZAMG's results page is mirrored to the VAST webpage (for an example see *Figure 8-1* and *Figure 8-2*).



VAST - MODEL

DISCLAIMER: These products are produced as part of the ESA research project VAST. They are published on this website for demonstration purposes. For official volcanic ash dispersion forecasts please refer to the corresponding Volcanic Ash Advisory Center (VAAC). For air traffic effects and flight status passengers should contact their national aviation authority and/or the airline companies directly. VAST refuses liability for any kind of use or misuse of the information published on this website.

LAST FINISHED EVENTS

Volcano Name	Simulation Begin	Calculation Finished	Species	Scenario	
Etna	05-12-2015 09:00		SO2	5: VAST Run	<a href="#">View</a>
Etna	04-12-2015 09:00		FASH	1: Real Case	<a href="#">View</a>
Etna	04-12-2015 06:00		FASH	5: VAST Run	<a href="#">View</a>
Etna	03-12-2015 00:00		SO2	5: VAST Run	<a href="#">View</a>
Etna	03-12-2015 00:00		None	1: Real Case	<a href="#">View</a>
Rinjani	02-12-2015 09:00		FASH	5: VAST Run	<a href="#">View</a>
Kanlaon	25-11-2015 00:00		FASH	5: VAST Run	<a href="#">View</a>
Sinabung	16-11-2015 06:00		FASH	5: VAST Run	<a href="#">View</a>
Rinjani	04-11-2015 00:00		FASH	5: VAST Run	<a href="#">View</a>
Sinabung	31-10-2015 06:00		FASH	5: VAST Run	<a href="#">View</a>

Figure 8-1: VAST website overview of events.

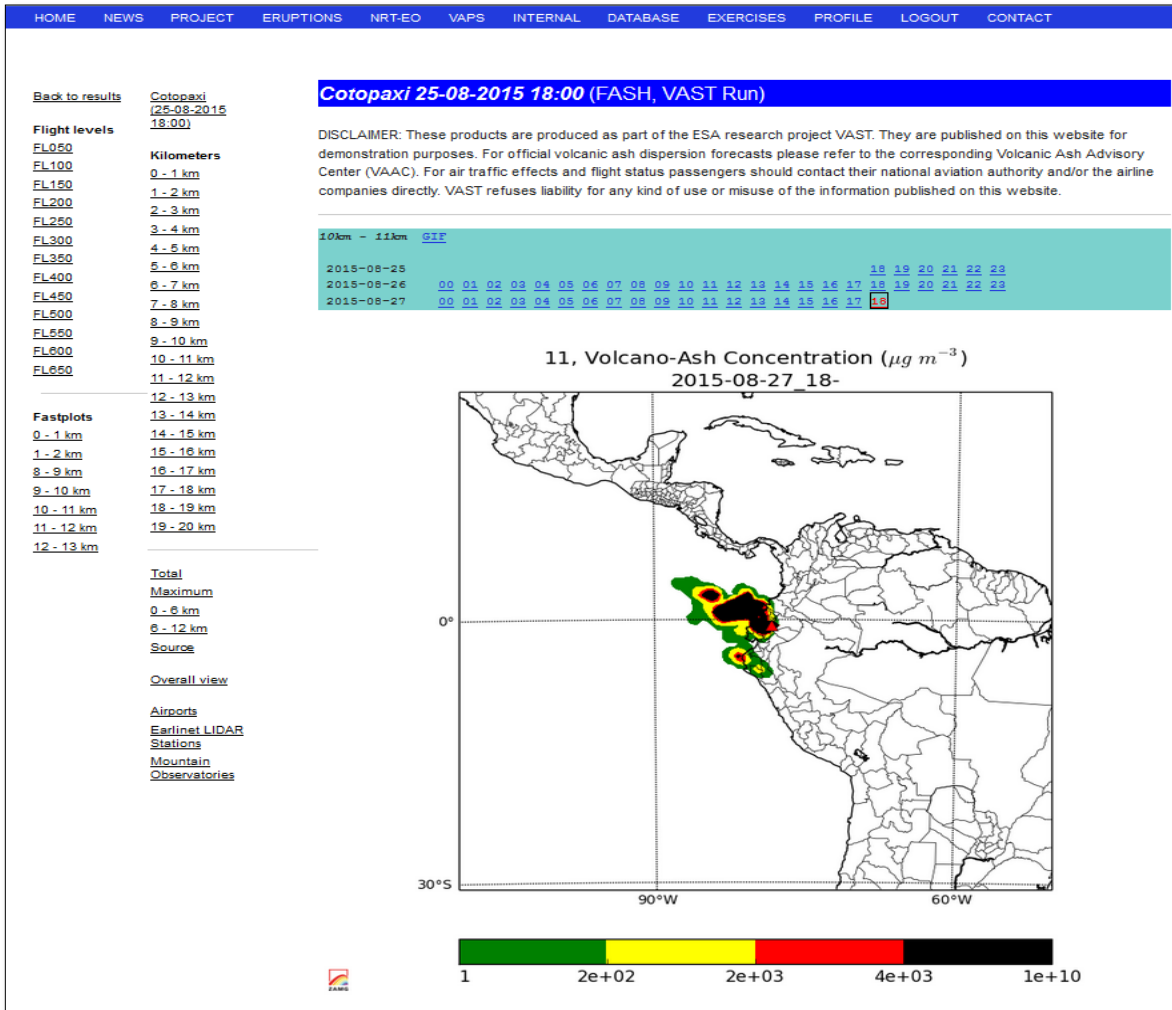


Figure 8-2: Example of the model forecasts transferred from ZAMG to NILU and mirrored at the VAST website.

## 8.2 Operational ensemble modelling service

A major outcome has been the introduction of the operational ensemble modelling system (see Chapter 4.3.2 Multi-input ensemble using ECMWF meteorological ensembles” for details). This mini-ensemble provides results of the maximum concentrations and probability plots (*Figure 8-3*) as well as time-height cross-sections for selected airports, LIDAR stations and mountain observatories (*Figure 8-4*).

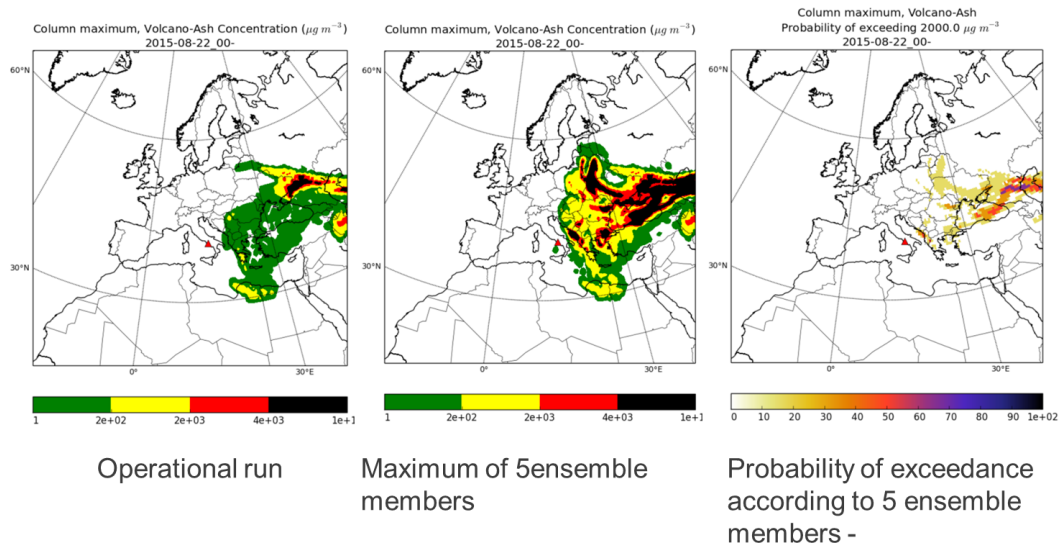


Figure 8-3: 2D output from the operational mini multi-input ensemble modelling with cluster analysis to find the representative members

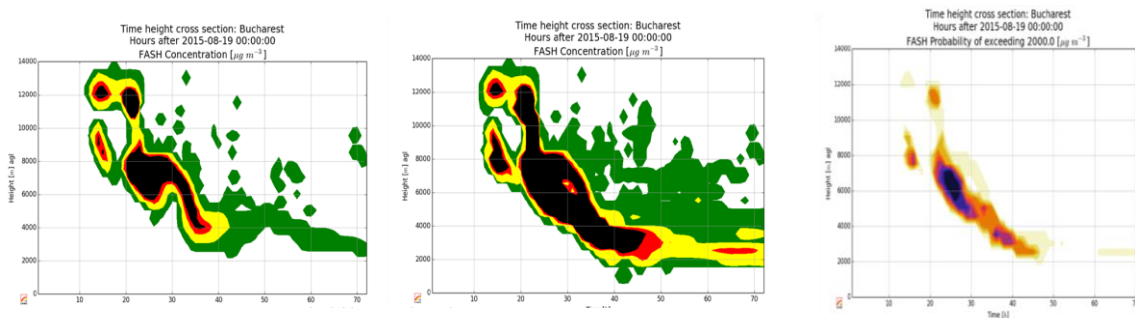


Figure 8-4: Time-height output from the operational mini multi-input ensemble modelling with cluster analysis to find the representative members.

### 8.3 Dynamical inverse modelling system

One of the objectives of VAST was to improve volcanic ash forecasts based on atmospheric dispersion and transport models by a seamless integration of inverse modelling. Given that the uncertainty of the source term is largely affecting the accuracy of the forecasts, constraining the source term with observations via inverse modelling in a near-real time basis is desirable. A **dynamic inverse modelling system**, capable of being run in near real-time, has been developed by the VAST-ZAMG team. The system includes structures to handle incoming satellite data and initialization of model simulations. As more satellite data become available, and also as more meteorological data become available for the model simulations, the system is re-run and the source term re-calculated and updated (*Figure 8-5*). Currently, SEVIRI satellite data are available quasi real-time, about 15-30 minutes behind real-time. Meteorological forecast data are available in real time, while analysis data have delays of up to 15 hours compared to real time. The system is re-run as new analysis/forecast data are available and

simulations based on analysis data replace those based on forecast data whenever analysis data become available. Data availability, computational time for pre-processing and running the system constrain the response time of the system. Typically, forecasts for the volcanic emissions based on the dynamic inversion system can be available 7 to 15 hours after the start of the eruptions and be updated every 6 to 12 hours. The technical implementation of the prototype system is completed by VAST. Additional optimization and testing of the system on a near-real time basis is required to ensure feasibility before the system can be implemented into an operational environment. In particular, the availability, quality and uncertainty estimates of the satellite data used for constraining the source term are essential and need to be adequately assigned. To date, only a few satellite ash retrieval data are freely available in near-real time, and well-characterized uncertainty estimates for the satellite retrieval data are to-date not available. However, with new data and improved retrieval algorithms from future missions, we expect these issues to be addressed, and the tool will then be more suitable for an operational implementation. Lastly, previous case-study experiences have shown that the set-up for one particular event does not necessarily provide meaningful results for other events. That means that, even in an operational dynamical inversion system, the results will need human expert analysis and adjustments in order to provide trustworthy results. More details on the system, including software requirements, is given in the VAST technical report (see *Arnold et al., 2015*).

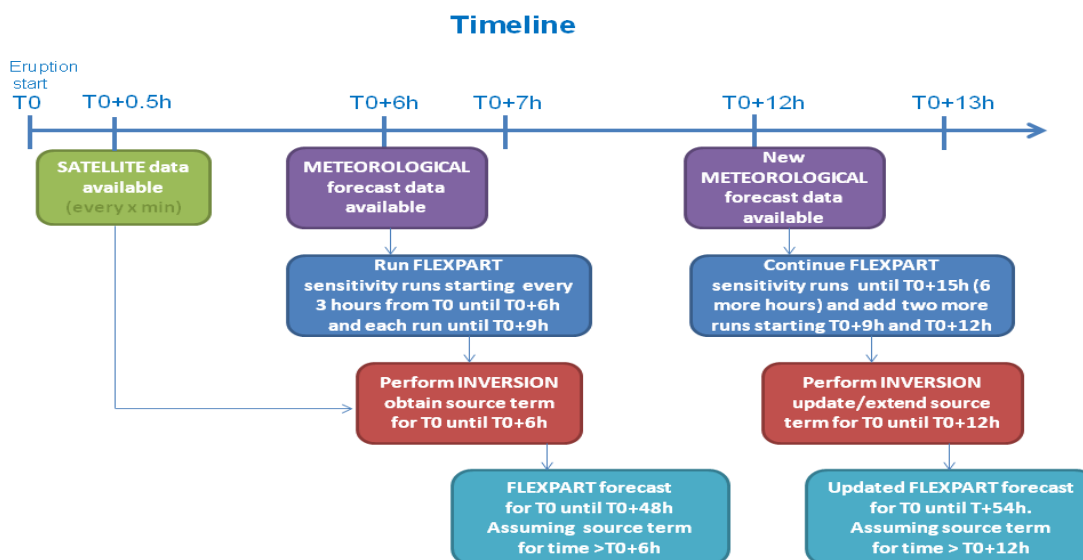


Figure 8-5: Diagram of the dynamic inversion system: the source-term calculations are re-run and updated as new satellite data and meteorological data are available.

## 8.4 Email notification service

The operational system is complemented with an e-mail notification system that takes information of different sources (SACS warnings, VAAC messages and NILU notifications) and filter the significant

events which are subsequently sent as notifications via email or phone the people in charge of the 24/7 forecasts and the members of the VAST project. An example of the email notification for the Calbuco eruption is shown below:

-----  
FILTERED WARNINGS GTS:  
-----

['DTG: 20150422/2300Z\r', 'VAAC: BUENOS AIRES\r', 'VOLCANO: CALBUCO 358020\r', 'AREA: CHILE\r', 'AVIATION COLOUR CODE: RED\r', 'ERUPTION DETAILS: EXPLOSIVE ERUPTION\r']

-----  
FILTERED WARNINGS SACS:  
-----

.... no new SACS

-----  
FILTERED WARNINGS VAST SACS:  
-----

.... no new VAST SACS

-----  
FILTERED WARNINGS VAST SACS ASH:  
-----

.... no new VAST SACS ASH

-----  
FILTERED WARNINGS NILU:  
-----

.... no new NILU

\*\*\*\*\*  
Links to be used for cross-checking:  
\*\*\*\*\*

VOLE and NILU warnings are very sensitive to Sahara dust events

-) Compared dust forecasts:

<http://sds-was.aemet.es/forecast-products/dust-forecasts/compared-dust-forecasts>

-) Official observatories/sites:

<http://www.volcano.si.edu/>

<http://www.ct.ingv.it/en/>

<http://en.vedur.is/#tab=skjalftar/>

-) Website with volcano news:

<http://www.volcanodiscovery.com/news.html>

## 9. THE IRISH LIDAR ASH DETECTION NETWORK

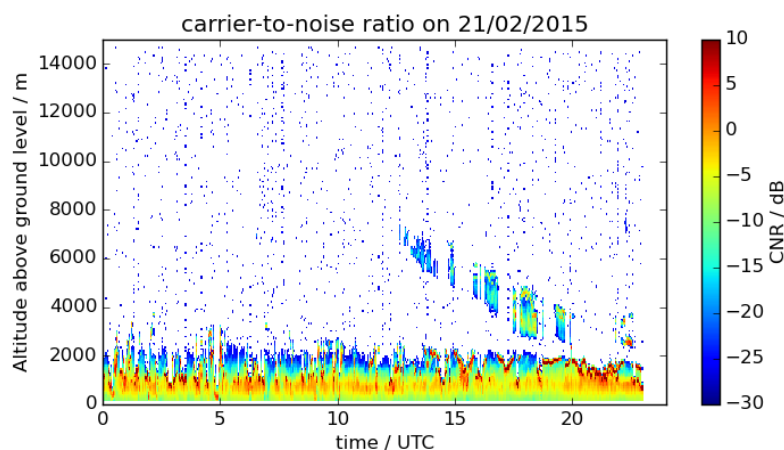
One of the objectives of VAST was to coordinate a LIDAR network for volcanic aerosol detection and model validation. LIDARs are active remote sensing instruments capable of delivering aerosol profiles in a high temporal and vertical resolution, which makes them powerful instruments for the detection of aerosol layers in the troposphere or even the lower stratosphere.

The Irish Aviation Authority (IAA) purchased three Raman LIDARs and planned to install them at three locations in Ireland, one at Malin Head in the North, one at Mace Head in the West and one on Mount Gabriel in the South. One one-wavelength LIDAR was already installed in Dublin. Unfortunately, the three Raman LIDARs (RMAN, manufacturer Leosphere) were faulty and could not be operated in a reliable way. They were therefore replaced by two Doppler wind LIDARs (Light Detection and Ranging) of the type WindCube 200S from Leosphere. The wind measurements depend on the presence of scatterers in form of cloud droplets or aerosol particles. The Doppler LIDAR is therefore also suited for the detection of aerosol layers, like volcanic ash plumes.

The first Doppler LIDAR was set up for automatic 24/7 operation at Mace Head at the west coast of Ireland in the end of December 2014. The second LIDAR is located at the Dublin airport. The wind and uncalibrated backscatter data of the WindCube are updated hourly at:

<http://macehead.nuigalway.ie/rt/LIDAR.html>

*Figure 9-1* shows an example of the LIDAR output. The carrier-to-noise ratio is related to the attenuated backscatter.



*Figure 9-1: Vertical profiles of the backscattered signal on 21 February 2015.*

A great advantage of the WindCube compared to conventional LIDARs is, that it is a scanning LIDAR. Therefore it does not only produce one vertical profile at a time, but can also be used to monitor the horizontal distribution of aerosols and clouds. In *Figure 9-2* a scan from 0 degrees elevation pointing North – over zenith – to 0 degrees elevation pointing south is shown. In this case, four different cloud layers were detected, at 1.8 km, 2.2 km, 3.5 km and between 7 and 8 km. The backscatter signal below 1.8 km and up to 8 km horizontal distance from the LIDAR was due to aerosols.

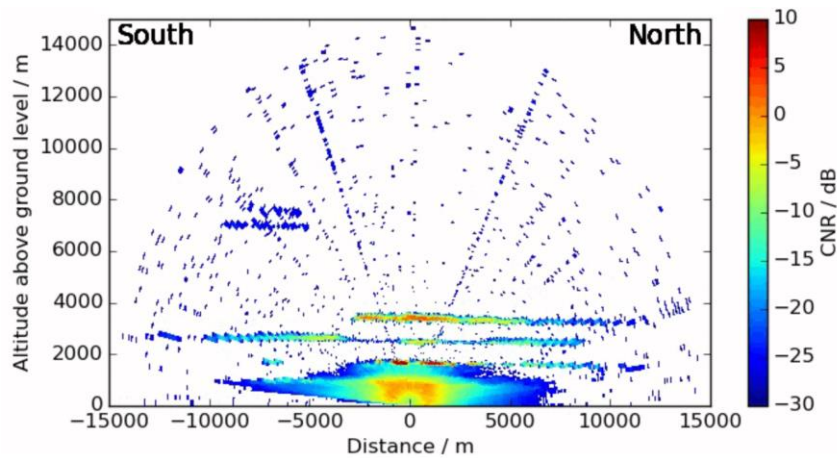


Figure 9-2: Backscattered signal from N-S scan over zenith on 21 February 2015 between 14 and 15 UTC.

### Combination of remote sensing instruments at Mace Head, Ireland

A feature mask was developed by combining continuous ceilometer and cloud radar measurements at Mace Head, Ireland. The product shows in near real time the presence of boundary layer aerosol, clouds, rain and lofted aerosol layers at Mace Head. Plots are available and updated every 15 minutes at: <http://macehead.nuigalway.ie/rt/feature.html>.

An example of the feature mask is shown in Figure 9-3. The data displayed was measured on 19 April 2010, shortly after the eruption of Eyjafjallajökull in Iceland. One lofted aerosol plume is visible from around 14 UTC. Back-trajectory analysis identified it as a volcanic ash layer, and ground-based in-situ measurements later confirmed this, after entrainment of the aerosol into the boundary layer. It was first detected at about 4 km height and descended with time. Besides, optically thinner layers in the free troposphere are visible earlier that day at lower altitudes in cloud-free periods.

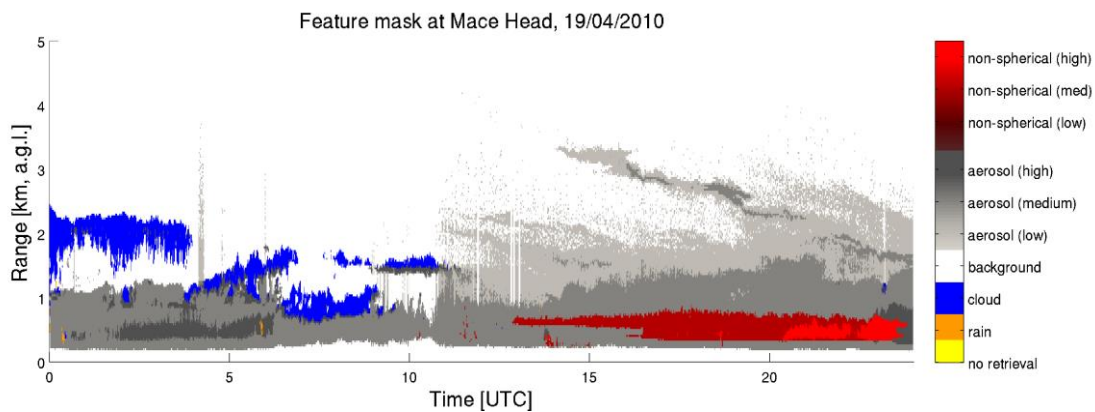


Figure 9-3: Feature mask on 19 April 2010, after the eruption of Eyjafjallajökull.



There is no discrimination made between local boundary layer aerosol and layers in the free troposphere. However, the depolarisation data of the cloud radar can be used to distinguish spherical from non-spherical particles. Volcanic ash is known to consist of non-spherical particles. However, the cloud radar is limited to the detection of large particles. Aerosol layers with sufficiently large non-spherical particles are classified as such (red scale in *Figure 9-3*). This does not mean, that all other aerosol layers consist only of spherical particles. It rather indicates, that the particles are too small to be detected by the radar. In the lower altitudes from around noon of the example case, non-spherical particles were detected by the cloud radar and the ceilometer. Their concentration increases with time, as more volcanic ash gets mixed down into the boundary layer.

The combination of the suite of remote sensing instruments at Mace Head and a Doppler LIDAR at Dublin enables the detection of free tropospheric aerosol and its transport over Ireland. With the closest volcanic sources being located in Iceland, Mace Head is a prime site for an early detection of volcanic aerosol plumes. This remote sensing data can be used to alert Ireland and Europe of volcanic aerosol advection in case of westerly and north-westerly winds.

## 9. CONCLUSIONS AND OUTLOOK

The ESA project VAST brought together teams from four European countries to improve the quality and use of satellite based observations in numerical atmospheric dispersion models for the purpose of assisting global aviation. Within the project, ash and SO<sub>2</sub> retrieval algorithms utilizing a number of satellite instruments, in particular SEVIRI, AIRS, MODIS, and AATSR, were developed and/or improved. VAST further developed improved transport modelling tools, based on the FLEXPART, SILAM, and WRF-Chem models, for predicting the transport of ash and SO<sub>2</sub> clouds in the atmosphere. Source term inversion was used for determining the source term of ash and SO<sub>2</sub> during volcanic eruptions, utilizing satellite observations as a constraint. Data assimilation was used for correcting errors in the transport model and ensemble modelling was used for inferring uncertainties. An operational demonstration service was set up to operate on a continuous basis for significant volcanic eruptions affecting the European air space and on a best-effort basis for worldwide events. Furthermore, a dynamic inverse modelling system prototype has been developed.

As a response to the requirement “R1 Access to all data sources of volcanic plume observations in Europe should be accelerated, improved and open” from *Zehner (2012)*, the VAST team compiled a benchmark test dataset for historic volcanic eruptions. In 2016, these datasets were transferred to the ESA Validation Data Centre (EVDC) for long term data access and archiving.

New satellite data products from the EO system are emerging. On February 16, 2016, the ESA/GMES Sentinel-3A satellite was launched successfully from Plesetsk, Russia, carrying on-board the Sea and Land Surface Temperature Radiometer (SLSTR) instrument. SLSTR has characteristics similar to AATSR, and the ash retrieval methods developed in VAST can be applied to SLSTR data. SLSTR will play an important role in quantitative ash remote sensing together with TropOMI on board Sentinel-5

precursor and the eagerly awaited Sentinel-4 mission, which will include an infrared sounder and UV instrument in geostationary orbit.

Inversion/data assimilation-based methods have become more widely used by several groups worldwide and dispersion models are subject to continuous development through a range of applications. For example, a new wet scavenging parameterization for aerosols was recently implemented in FLEXPART. Nevertheless, important volcanic processes, for example ash aggregation and entrainment of water, are still not being included in the operational dispersion models and also in many research-mode models. Further optimization and testing of the VAST-developed dynamic inverse modelling system prototype on a near-real time basis is required before implemented into an operational environment. Based on experiences made with a limited number of case studies, it is expected that the results will need some human expert analysis and adjustments in order to provide optimal results. It is important to test and verify that new developments continue to give optimized results for volcanic ash forecasting. As such, participation in exercises such as the internationally coordinated VOLCEX, is desirable.

VAST brought together a suite of techniques for aiding aviation in case of volcanic eruptions, including satellite and ground-based observations and modelling approaches. Methods were developed, improved and tested thoroughly, and integrated into an operational demonstration service. Still there remain many questions about the validity of satellite retrievals, the error characteristics, the timeliness and paucity of validation data with which to corroborate and validate the satellite estimates. Furthermore, a coordinated inverse/data assimilation-modelling intercomparison study, focussing on volcanic ash forecasting, seems desirable to streamline the development and validation of more robust operational methods for volcanic ash forecasting, and identify weaknesses of the current operational systems.

Sustainable tools developed during VAST will support the project partners in their role/mandate in helping national authorities in a future volcanic ash crisis situation. ESA support for VAST, as well as for the sister-projects SACS and SMAH, leaves European institutions and users better prepared to monitor and forecast hazardous volcanic ash and SO<sub>2</sub> plumes in the European and global airspace.

## 10. BIBLIOGRAPHY

The following **VAST deliveries**: reports, ATBDs and Technical Notes can be found on the VAST project webpage (see <http://vast.nilu.no/project/deliverables/>).

- Aas et. al. (2012), VAST User Requirement Document, v0.4, ESA-VAST document, NILU-ESA-VAST-URD-v0.4, Oslo, Norway, 17 December 2012.
- Arnold, D., C. Maurer, N.I. Kristiansen, and E. Sollum (2014), Technical report on NRT determination of source terms of SO<sub>2</sub> and ash: Part 2. VAST Ad-hoc inversion HOWTO, ESA-VAST document, v3.0, 22pp, April 2014.
- Kristiansen, N. I., A. Stohl, G. Wotawa, M. Sofiev., J. Vira., D. Martin., and Colin O'Dowd (2014), Modelling of volcanic ash and SO<sub>2</sub>, Algorithm Theoretical Basis Document, ESA-VAST document, NILU, v3, pp 44, 22 April 2014.
- Kristiansen, N. I., A. Stohl and D. Arnold (2014), Technical report on NRT determination of source terms of SO<sub>2</sub> and ash: Part 1: Procedures for volcano inversions using FLEXPART, ESA-VAST document, v6.3, NILU, 39pp, April 2014.
- Kylling A. and F. Prata (2013), Moderate Resolution Imaging Spectroradiometer (MODIS) Algorithm Theoretical Basis Document. ESA-VAST document, NILU, 25 pp, May 2013.
- O'Dowd, C., Product validation report, v1.4, ESA-VAST document, Galway, 68 pp, February 2016.
- Prata, A. J. (2013), Detecting and Retrieving Volcanic Ash from SEVIRI Measurements. Algorithm Theoretical Basis Document, ESA-VAST document, NILU, 55 pp., May 2013.
- Prata, A. J. (2013), A Volcanic Ash Detection Algorithm Using AIRS Brightness Temperatures, Algorithm Theoretical Basis Document, ESA-VAST document, NILU, 14pp, May 2013.
- Prata, F., Zehner, C., Stebel, K. (2014), Earth observations and volcanic ash. A report from the ESA/Eumetsat Dublin workshop, 4-7 March, 2013. Frascati, European Space Agency (doi:10.5270/atmva-14-04).
- Stebel, K., Kristiansen, N. and E. Sollum (2015), VAST Database Description, vers 3.0, ESA-VAST document, NILU, 21 pp, September 2015.
- Virtanen, T., P. Kolmonen, and G. de Leeuw (2013), AATSR VIS/NIR AOD Retrieval, Algorithm Theoretical Basis Document. VAST document, FMI, DRAFT version 1.0, 31pp, Dec. 2013.
- Virtanen, T., and G. de Leeuw (2013), AATSR Plume Top Height Estimate, Algorithm Theoretical Basis Document, VAST document, FMI, DRAFT version 1.0., 35pp., Dec. 2013.
- Virtanen, T.H. and G. de Leeuw (2015), Use of operational EO data report, ESA-VAST document, FMI, 18 pp., Sept 2015.

A number of **peer reviewed publications** and two **master thesis** were written during VAST.

- Klonner, R. (2013), Clustering ECMWF ENS ensemble predictions to optimise FLEXPART plume dispersion ensembles. Masher thesis.
- Kristiansen, N. I., A. Stohl, F. Prata, N. Bukowiecki, H. Dacre, S. Eckhardt, S. Henne, M. Hort, B. Johnson, F. Marengo, B. Neining, O. Reitebuch, P. Seibert, D. Thomson, H. Webster, B. Weinzierl (2012), Performance assessment of a volcanic ash transport model mini-ensemble used for inverse modelling of the 2010 Eyjafjallajökull eruption, *J. Geophys. Res.*, 117, D00U11, doi:10.1029/2011JD016844.
- Kristiansen, N. I., D. Arnold, C. Maurer, J. Vira, R. Rădulescu, D. Martin, A. Stohl, K. Stebel, M. Sofiev, C. O' Dowd, G. Wotawa (2015) : Improving model simulations of volcanic emission clouds and assessing model uncertainties, 07-Sept-2015, accepted for publication in AGU Monograph: Natural Hazard Uncertainty Assessment by eds: P. Webley and others.

- Kristiansen, N.I., A.J. Prata, A. Stohl, and S. A. Carn (2015), Stratospheric volcanic ash emissions from the 13 February 2014 Kelut eruption, *Geophys. Res. Lett.*, 42, 588–596, doi:10.1002/2014GL062307.
- Moxnes, E. D., N. I. Kristiansen, A. Stohl, L. Clarisse, A. Durant, K. Weber, and A. Vogel (2014), Separation of ash and sulfur dioxide during the 2011 Grímsvötn eruption, *J. Geophys. Res. Atmos.*, 119, doi:10.1002/2013JD021129.
- Moxnes E. D. (2013), Estimating the sulphur dioxide and ash emissions from the Grímsvötn 2011 volcanic eruption and simulating their transport across Northern Europe, Master Thesis, University of Oslo, June 2013.
- Prata, A. J. and A. T. Prata (2012), Eyjafjallajökull ash concentrations determined using SEVIRI measurements, *J. Geophys. Res. (Atmospheres)*, 117, D00U23, doi:10.1029/2011JD016800.
- Stohl, A., A. J. Prata, S. Eckhardt, L. Clarisse, A. Durant, S. Henne, N. I. Kristiansen, A. Minikin, U. Schumann, P. Seibert, K. Stebel, H. E. Thomas, T. Thorsteinsson, K. Tørseth, and B. Weinzierl (2011), Determination of time- and height-resolved volcanic ash emissions for quantitative ash dispersion modeling: The 2010 Eyjafjallajökull eruption, *Atmos. Chem. Phys.*, 11, 4333–4351, doi:10.5194/acp-11-4333-2011.
- Virtanen, T. H., Kolmonen, P., Rodríguez, E., Sogacheva, L., Sundström, A.-M., and de Leeuw, G. (2014), Ash plume top height estimate using AATSR, *Atmos. Meas. Tech.*, 7, 2437–2456, doi:10.5194/amt-7-2437-2014.

## REFERENCES

- Aas et. al. (2012), VAST User Requirement Document, v0.4, ESA-VAST document, NILU-ESA-VAST-URD-v0.4, Oslo, Norway, 17 December 2012.
- Chahine, M. T., et al., (2006) AIRS: Improving weather forecasting and providing new data on greenhouse gases, *Bull. Am. Meteorol. Soc.*, 87(7), 911–926, doi:10.1175/BAMS-87-7-911.
- Clarisse, L., Prata, A. J., Lacour, J.-L., Hurtmans, D., Clerbaux, C., and P.-F. Coheur, (2010), A correlation method for volcanic ash detection using hyperspectral infrared measurements, *Geophys. Res. Lett.*, 37, L19806, doi:10.1029/2010GL044828.
- Donlon, C., Berruti, B., Buongiorno, A., Ferreira, M.-H., Féménias, P., Frerick, J., Goryl, P., Klein, U., Laur, H., Mavrocordatos, C., Nieke, J., Rebhan, H., Seitz, B., Stroede, J., Sciarra, R. (2012), The Global Monitoring for Environment and Security (GMES) Sentinel-3 Mission, *Remote Sensing of the Environment*, 120, 27-57, doi: 10.1016/j.rse.2011.07.024.
- EVACEG (2010) European Volcanic Ash Cloud Experts Group (EVACEG), Recommendations for the Improvement of Volcanic Ash Cloud Crisis Prevention and Management; Report to the Spanish EU Presidency, June 2010, 27 p.
- Galmarini, S., R. Bianconi, W. Klug, T. Mikkelsen, R. Addis, S. Andronopoulos, P. Astrup, A. Baklanov, J. Bartniki, J.C. Bartzis, R. Bellasio, F. Bompay, R. Buckley, M. Bouzom, H. Champion, R. D'Amours, E. Davakis, H. Eleveld, G.T. Geertsema, H. Glaab, M. Kollax, M. Ilvonen, A. Manning, U. Pechinger, C. Persson, E. Polreich, S. Potemski, M. Prodanova, J. Saltbones, H. Slaper, M.A. Sofiev, D. Syrakov, J.H. Sørensen, L. Van der Auwera, I. Valkama, R. Zelazny (2004), Ensemble dispersion forecasting—Part I: concept, approach and indicators, *Atmospheric Environment*, 38, 28, 4607–4617, doi:10.1016/j.atmosenv.2004.05.030.
- Gangale, G., Prata, A. J., and Clarisse, L., (2010), The infrared signature of volcanic ash determined from high-spectral resolution measurements, *Rem. Sensing Environ.*, 114, 414–425, doi:10.1016/j.rse.2009.09.007.
- Kolmonen, P., Sogacheva, L., Virtanen, T.H., de Leeuw, G., and Kulmala, M. (2015), The ADV/ASV AATSR aerosol retrieval algorithm: current status and presentation of a full-mission AOD dataset, *International Journal of Digital Earth*, DOI: 10.1080/17538947.2015.1111450.

- Kylling A. and F. Prata (2013), Moderate Resolution Imaging Spectroradiometer (MODIS) Algorithm Theoretical Basis Document. ESA-VAST document, NILU, 25 pp, May 2013.
- Mastin, L.G., Guffanti, Marianne, Ewert, J.E., and Spiegel, Jessica, 2009, Preliminary spreadsheet of eruption source parameters for volcanoes of the world: U.S. Geological Survey Open-File Report 2009-1133, v. 1.2, 25 p. [<http://pubs.usgs.gov/of/2009/1133/>].
- O'Dowd, C., Product validation report, v1.4, ESA-VAST document, Galway, 68 pp, February 2017.
- Oxford Economics (2010), The economic impacts of air travel restrictions due to volcanic ash, Report prepared for Airbus, 12pp, Available from: [www.oxfordeconomics.com](http://www.oxfordeconomics.com).
- Pollack, J. B., O. B. Toon, B. N. Khare (1973), Optical properties of some terrestrial rocks and glasses, *Icarus*, 19, 3, doi:10.1016/0019-1035(73)90115-2.
- Prata, A. J. (1989), Radiative transfer calculations for volcanic ash clouds, *Geophys. Res. Lett.*, 16(11), 1293-1296, 1989.
- Prata, F, G. Bluth, B. Rose, D. Schneider, and A. Tupper (2001), Comments on "Failures in detecting volcanic ash from a satellite-based technique", *Remote Sensing of Environment* 78 (3), 341-346, doi:10.1016/S0034-4257(01)00231-0.
- Prata, A. J. and C. Bernardo (2007), Retrieval of volcanic SO<sub>2</sub> column abundance from Atmospheric Infrared Sounder data, *J. Geophys. Res.*, 112, D20204, doi: 10.1029/2006JD007955
- Prata, A. J. (2008), Satellite detection of hazardous volcanic clouds and the risk to global air traffic, *Natural Hazards*, DOI 10.1007/s11069-008-9273-z.
- Prata, F. and S. Corradini (2009), Algorithm Theoretical Basis Document: Infrared Sulphur Dioxide Algorithms, ESA-SAVAA document, NILU, 118 pp, September 2009. (<http://savaa.nilu.no/PublicArchive/tabid/3207/Default.aspx>).
- Prata, A. J., and A. T. Prata (2012), Eyjafjallajökull volcanic ash concentrations determined using Spin Enhanced Visible and Infrared Imager measurements, *J. Geophys. Res.*, 117, D00U23, doi:10.1029/2011JD016800.
- Prata, A. J. (2013), Detecting and Retrieving Volcanic Ash from SEVIRI Measurements. Algorithm Theoretical Basis Document, ESA-VAST document, NILU, 55 pp., May 2013.
- Prata, A. J. (2013), A Volcanic Ash Detection Algorithm Using AIR Brightness Temperatures, Algorithm Theoretical Basis Document, ESA-VAST document, NILU, 14pp, May 2013.
- Prata, F., Zehner, C., Stebel, K. (2014), Earth observations and volcanic ash. A report from the ESA/Eumetsat Dublin workshop, 4-7 March, 2013. Frascati, European Space Agency [doi:10.5270/atmva-14-04] [http://vast.nilu.no/media/documents/internal/2014/04/27/dublinreport\\_v3.0-print.pdf](http://vast.nilu.no/media/documents/internal/2014/04/27/dublinreport_v3.0-print.pdf).
- Stebel, K., Kristiansen, N. and E. Sollum (2015), VAST Database Description, vers 4.0, ESA-VAST document, NILU, 21 pp, February 2016.
- Virtanen, T. H., Kolmonen, P., Rodríguez, E., Sogacheva, L., Sundström, A.-M., and de Leeuw, G. (2014), Ash plume top height estimate using AATSR, *Atmos. Meas. Tech.*, 7, 2437-2456, doi:10.5194/amt-7-2437-2014.
- Virtanen, T., P. Kolmonen, and G. de Leeuw (2013), AATSR VIS/NIR AOD Retrieval, Algorithm Theoretical Basis Document. VAST document, FMI, DRAFT version 1.0, 31pp, Dec. 2013.
- Virtanen, T., and G. de Leeuw (2013), AATSR Plume Top Height Estimate, Algorithm Theoretical Basis Document, VAST document, FMI, DRAFT version 1.0., 35 pp., Dec. 2013.
- Zehner, C., Ed. (2012) Monitoring Volcanic Ash from Space. ESA - EUMETSAT workshop on the 14 April to 23 May 2010 eruption at the Eyjafjöll volcano, South Iceland (ESA/ESRIN, 26 -27 May 2010), ESA Publication STM-280. doi: 10.5270/atmch-10-01.